AMRL-TR-75-12

SEARCH TECHNIQUES FOR SELF-ORGANIZING SYSTEMS

ADAPTRONICS, INC.
WESTGATE RESEARCH PARK
7700 OLD SPRINGHOUSE ROAD
McLEAN, VIRGINIA 22101

JULY 1975

AEROSPACE MEDICAL RESEARCH LABORATORY
AEROSPACE MEDICAL DIVISION
Air Force Systems Command
Wright-Patterson Air Force Base, Ohio 45433

NOTICES

When US Government drawings, specifications, or other data are used for any purpose other than a definitely related Government procurement operation, the Government thereby incurs no responsibility nor any obligation whatsoever, and the fact that the Government may have formulated, furnished, or in any way supplied the said drawings, specifications, or other data, is not to be regarded by implication or otherwise, as in any manner licensing the holder or any other person or corporation, or conveying any rights or permission to manufacture, use, or sell any patented invention that may in any way be related thereto.

Organizations and individuals receiving announcements or reports via the Aerospace Medical Research Laboratory automatic mailing lists should submit the addressograph plate stamp on the report envelope or refer to the code number when corresponding about change of address or cancellation.

Do not return this copy. Retain or destroy.

Please do not request copies of this report from Aerospace Medical Research Laboratory. Additional copies may be purchased from:

National Technical Information Service
5285 Port Royal Road
Springfield, Virginia 22151

This report has been reviewed and cleared for open publication and/or public release by the appropriate Office of Information (OI) in accordance with AFR 190-17 and DODD 5230.0. There is no objection to unlimited distribution of this report to the public at large, or by DDC to the National Technical Information Service (NTIS).

This technical report has been reviewed and is approved for publication.

FOR THE COMMANDER

Henning E. von Gierke

HENNING E. VON GIERKE
Director
Biodynamics and Bionics Division
Aerospace Medical Research Laboratory

ACCESSION for		
NTIS	White Section	✓
DDC	Buff Section	☐
UNANNOUNCED		☐
JUSTIFICATION........		
BY........		
DISTRIBUTION/AVAILABILITY CODES		
Dist.	AVAIL. and/or SPECIAL	
A		

Dr. Hedma... Rpt.
AD-A014 174

SECURITY CLASSIFICATION OF THIS PAGE (When Data Entered)

REPORT DOCUMENTATION PAGE

READ INSTRUCTIONS BEFORE COMPLETING FORM

1. REPORT NUMBER: AMRL-TR-75-12
2. GOVT ACCESSION NO.
3. RECIPIENT'S CATALOG NUMBER
4. TITLE (and Subtitle): SEARCH TECHNIQUES FOR SELF-ORGANIZING SYSTEMS
5. TYPE OF REPORT & PERIOD COVERED: Final Technical Report 8/15/73 - 10/15/74
6. PERFORMING ORG. REPORT NUMBER: 682
7. AUTHOR(s): Elizabeth R. Johnson; Anthony N. Mucciardi, Ph.D.
8. CONTRACT OR GRANT NUMBER(s): F33615-74-C-4007
9. PERFORMING ORGANIZATION NAME AND ADDRESS: ADAPTRONICS, INC. Westgate Research Park 7700 Old Springhouse Road McLean, Virginia 22101
10. PROGRAM ELEMENT, PROJECT, TASK AREA & WORK UNIT NUMBERS: 61102F, 7232-01-05
11. CONTROLLING OFFICE NAME AND ADDRESS: Aerospace Medical Research Laboratory Air Force Systems Command Wright-Patterson Air Force Base, Ohio
12. REPORT DATE: July 1975
13. NUMBER OF PAGES: 79
14. MONITORING AGENCY NAME & ADDRESS (if different from Controlling Office)
15. SECURITY CLASS (of this report): UNCLASSIFIED
15a. DECLASSIFICATION DOWNGRADING SCHEDULE
16. DISTRIBUTION STATEMENT (of this Report)

Approved for public release; distribution unlimited

D D C
SEP 12 1975
D

17. DISTRIBUTION STATEMENT (of the abstract entered in Block 20, if different from Report)
18. SUPPLEMENTARY NOTES
19. KEY WORDS (Continue on reverse side if necessary and identify by block number)

Self-Organizing Systems
Bionics
Artificial Intelligence
Goal-Seeking Systems
Search Techniques

20. ABSTRACT (Continue on reverse side if necessary and identify by block number)

This study has been devoted to extension and further development of search algorithms of utility for self-organizing control systems. The four major results of this study are as follows:

Self-organizing search methods developed in the previous study (AMRL-TR-73-76) have been extended to higher-dimensional multimodal problems and have been shown to be very effective.

DD FORM 1473 1 JAN 73 EDITION OF 1 NOV 65 IS OBSOLETE

20. A composite search algorithm incorporating both the pdf guided search and the guided accelerated random search was found to be more effective than either search algorithm alone.

Clustering analysis has been shown to be a valuable tool for assessing the complexity of a search surface. The number of modes (peaks), their locations relative to each other, their shape and volume, and the estimated maximum performance value within each are all adaptively determined via clustering.

A new method for image encoding has been formulated that provides image reconstruction of similar quality to methods currently in use. This procedure also can find regions of possible interest within the image because of its ability to treat the image as a whole rather than line-by-line. This characteristic considerably enhances its value as a tool in image pattern recognition and classification.

PREFACE

This report was prepared for the United States Air Force, Air Force Systems Command, by Adaptronics, Inc. under the terms of contract F33615-74-C-4007, "Self-Organizing Systems Theory for the Development of Weapons Systems." The report covers work performed during the period 15 August 1973 to 15 October 1974.

The Project Engineer for the Air Force has been Dr. Hans L. Oestreicher, Chief, Mathematics and Analysis Research, Aerospace Medical Research Laboratory. The authors thank Dr. Oestreicher for his encouragement and assistance in the program.

Dr. Anthony N. Mucciardi was Project Manager and Principal Investigator for Adaptronics. The authors thank Mr. Ramesh Shankar of the Adaptronics staff for technical assistance in the image processing task, and Mr. Richard Wren of Washington University (St. Louis) for providing the digitized image.

CONTENTS

TABLES

FIGURES

SECTION I

INTRODUCTION

This project is a continuation of the research begun under Contract F33615-73-C-4007 to investigate areas of self-organizing systems theory that are relevant to the Air Force. The previous study emphasized techniques for terminal-value control of vehicles and for control systems that must avoid operating regions with high performance penalties (11). Both cases required the development and incorporation of long-term memory in the parameter search algorithm. This memory was efficiently encoded in the form of multimodal probability density functions (pdf's).

The objective of the present project was to develop these techniques further and to extend them to higher-dimensional problems. Four major areas of interest were investigated. First, methods were developed and tested for increasing convergence rates of searches that must avoid high-penalty regions. Second, techniques for controlling probability density function-guided searches were refined. Third, use of clustering analyses to aid in determining the complexity of an optimization problem was studied further. Fourth, the strategies resulting from the above investigations were applied to an image-processing problem with potential application in remotely-piloted vehicle (RPV) ground target acquisition.

It was found that probability density function-guided searches can provide good information with which to initiate guided, accelerated random searches. The increased knowledge about the characteristics of the optimization problem that the pdf-guided search provides can be used to help other searches avoid regions of high resource consumption or disastrously low performance. Additionally, the pdf-guided search supplies a list of locations with high associated performance that can be used as starting points for subsequent searching.

Clustering analyses proved to be useful tools in locating and describing both local and global extrema, thus enabling the investigator to judge the complexity of the surface to be studied. In addition, they indicate shifts in extrema due to the interaction of the independent variables.

One of the major tasks of the RPV man-machine interface is the encoding, transmission, reconstruction, and interpretation of pictorial information. This is usually accomplished by fast Fourier encoding/decoding techniques. One main purpose of the remote pilot is to spot those regions of a picture that contain "interesting" information; e.g., a truck moving in a background of clutter. A disadvantage of the fast Fourier method is that it is insensitive to "interesting" regions; it treats all data equally. A novel application of the parameter search procedures studied in this project was made to this image interpretation problem. While the data compression and reconstruction properties of this new approach compare favorably to the fast Fourier method, the key result is that interesting regions of a picture are automatically identified by the new encoding process and conveyed directly to the remote pilot. Therefore, this approach showed good promise as a new technique for image encoding/decoding/interpretation. Although these procedures require further development, they indicate solid potential for equalling or bettering techniques presently in use.

SECTION II

DESCRIPTION OF NUMERICAL OPTIMIZATION TEST SURFACE

The first three (of four) work tasks in this project utilized the same performance function to test the parameter search algorithms. The function consists of a weighted sum of five Gaussianly-shaped modes, with centers as listed in Table 1. The location of each mode center remains constant for all values of NDIM; e.g., the first coordinate location of Mode 2 is always at 0.40. However, both the size factors of each mode, listed in Table 2, and the amplitude factors, listed in Table 3, are altered as the dimensionality of the parameter space (NDIM) is increased. It was necessary to broaden the five performance modes as NDIM and, consequently, the volume of the performance space was increased. This insured that all portions of the space would be influenced by at least one of the modes. The absolute amplitudes of the three smallest performance modes were increased for values of NDIM $\geq$ 10. In this way, most of the parameter space had a reasonably large (performance) functional value. As a result of these alterations in size and in amplitude, the location and function value of the global maximum shifts as NDIM changes, as shown in Table 4.

The performance test function value, f(X), for a point in the NDIM-dimensional hyperspace, $X = x_1, \ldots, x_{NDIM}$, is:

$$f(X) = f(x_1, \ldots, x_{NDIM}) = \sum_{m=1}^{5} w_m \, g_m(X)$$

where, $g_m(X)$ is the m^{th} Gaussian mode and it is equal to:

$$g_m(X) = \left[(2\Pi)^{NDIM/2} \left(\prod_{i=1}^{NDIM} \sigma_{mi}^2 \right)^{\frac{1}{2}} \right]^{-1} \times \exp\left[-\tfrac{1}{2} \sum_{i=1}^{NDIM} \left(\frac{x_i - \mu_{mi}}{\sigma_{mi}} \right)^2 \right]$$

where, μ_{mi}, σ_{mi} and w_m are given in Tables 1, 2, and 3, respectively.

TABLE 1

CENTERS OF MODES FOR PERFORMANCE TEST FUNCTION

Dimension	Mode 1	2	3	4	5
1	.80	.40	-.69	-.83	-.67
2	.39	-.82	-.98	.53	-.05
3	-.68	.59	.61	.03	-.18
4	.94	.49	-.72	.10	.75
5	-.20	-.62	.69	.79	-.86
6	.14	.56	.12	.74	.25
7	-.58	-.29	.41	.64	-.77
8	.30	.29	.81	-.04	-.39
9	-.80	.84	.09	.68	.54
10	.97	.18	-.03	.08	-.12
11	-.32	.42	-.66	-.01	.50
12	.19	.37	.98	.21	-.53
13	-.[illegible]	-.09	-.78	1.00	.55
14	.96	-.50	.99	-.75	.32
15	-.54	-.52	-.45	-.59	-.92
16	-.63	.67	.46	-.07	-.73
17	-.26	-.99	.77	.92	.32
18	-.14	-.19	-.74	-.47	-.94
19	-.76	-.27	.45	-.43	.17
20	.20	-.96	.62	-.81	.63

TABLE 2

SIZE FACTORS OF MODES FOR PERFORMANCE TEST FUNCTION

N	Dimension	Mode 1	Mode 2	Mode 3	Mode 4	Mode 5
2	1	.350	.400	.250	.700	.310
	2	.455	.175	.425	.200	.250
5	1	.600	.650	.750	.700	.550
	2	.705	.600	.675	.650	.750
	3	.760	.650	.680	.720	.710
	4	.700	.600	.685	.640	.610
	5	.690	.800	.710	.685	.770
10	1	.900	.850	.850	.900	.850
	2	1.005	.800	.775	.850	1.050
	3	1.060	.850	.780	.920	1.010
	4	1.000	.800	.785	.840	.910
	5	.890	1.000	.810	.885	1.070
	6	.900	.955	.775	.795	.850
	7	.870	.700	.800	.750	.860
	8	.900	.830	.785	.830	1.015
	9	.940	.940	.650	.935	.900
	10	.865	.800	.785	.920	.960
15	1	1.757	2.008	1.255	3.514	1.536
	2	2.284	.879	2.134	1.004	1.280
	3	1.280	2.008	1.079	1.180	1.178
	4	1.330	1.757	.728	.979	.947
	5	1.104	2.761	1.155	1.079	2.662
	6	1.757	1.832	.176	2.108	1.434
	7	2.209	1.054	1.506	.628	1.894
	8	1.004	1.355	2.259	2.761	2.176
	9	1.406	2.510	1.481	1.355	2.330
	10	1.079	1.305	2.761	2.033	1.178
	11	.929	2.259	1.807	2.008	1.178
	12	1.456	1.029	1.506	2.259	1.510
	13	1.205	2.284	.628	1.180	1.792
	14	2.385	3.514	2.284	1.205	1.229
	15	2.761	3.514	1.506	.954	1.280
20	1	2.815	3.217	2.010	5.629	2.432
	2	3.659	1.407	3.418	1.608	2.030
	3	2.051	3.217	1.729	1.890	1.870
	4	2.131	2.775	1.166	1.568	.151
	5	1.769	4.423	1.850	1.729	4.202
	6	2.815	2.935	2.815	3.337	2.272
	7	3.538	1.683	2.412	1.005	2.995
	8	1.608	2.171	3.613	4.423	3.438
	9	2.252	4.021	2.372	2.171	3.679
	10	1.729	2.091	[illegible]	3.257	1.870
	11	1.488	3.613	[illegible]	3.217	1.870
	12	2.332	1.649	[illegible]	3.619	2.392
	13	1.930	3.659	[illegible]	1.890	2.835
	14	3.820	5.629	[illegible]	1.930	1.959
	15	4.423	5.629	[illegible]	1.528	2.030
	16	1.649	1.769	[illegible]	2.131	1.870
	17	2.734	2.815	2.031	1.809	2.392
	18	1.287	1.769	2.412	1.608	3.558
	19	1.608	1.890	5.629	1.809	3.438
	20	1.005	2.332	1.045	2.412	3.247

TABLE 3

AMPLITUDE FACTORS OF MODES FOR PERFORMANCE TEST FUNCTION

N Dimension	Mode 1	2	3	4	5
2	-1.00	-0.50	0.10	0.50	1.00
5	-1.00	-0.50	0.10	0.50	1.00
10	-1.00	-0.75	0.50	0.75	1.00
15	-1.00	-0.75	0.55	0.75	1.00
20	-1.00	-0.75	0.55	0.75	1.00

TABLE 4

LOCATIONS AND FUNCTION VALUES OF GLOBAL MAXIMUM

Dimension	NDIM 2	5	10	15	20
1	-.671	-.710	-.734	-.848	-.976
2	-.046	-.025	-.014	.463	.486
3		-.187	-.237	-.063	-.056
4		.746	.755	.390	.745
5		-.855	-.859	.653	.660
6			.246	.423	.377
7			-.788	.561	.535
8			-.442	-.537	-1.000
9			.543	.705	.835
10			-.154	-.145	-.312
11				.420	.595
12				-.446	-.734
13				.939	-.879
14				-.292	-.181
15				-.693	-.734
16					-.640
17					.817
18					-.819
19					-.142
20					-.481
Function Maximum:	1.0164	.9696	.9459	.9660	1.0259

SECTION III
SELF-ORGANIZING SEARCH ALGORITHMS

It was shown in the previous work (11, 12, 13) that the results of a pdf-guided search could supply a good location from which to begin a guided random search -- at least for two-dimensional spaces. One of the work tasks in this project was to investigate this concept for higher dimensional spaces. By way of introduction, the next two subsections are excerpted from (11).

3.1 Self-Organizing Long-Term Memory Search (PDF)

Because of physiological, structural, thermal, or other constraints, many systems must avoid operating regions characterized by very high performance penalties. Those cases in which the regions to be avoided can be excluded by placing *a priori* bounds on the search present little difficulty; therefore, the other cases, in which these regions can only be determined after the fact, were investigated in this study.

The two types of high-penalty search problems are:

1. Those in which a particular choice of a set of parameters leads to poor system performance (as measured by a performance assessment function) with an accompanying large consumption of system resources (e.g., operating an aircraft engine well below its maximum thermodynamic efficiency decreases its work output and increases the fuel consumption).
2. Those in which a particular choice of a set of parameter leads to a disastrous outcome (e.g., increasing the pressure in a boiler beyond an upper safety limit).

Since the resources available to conduct the parameter search problem are limited (such as the amount of aircraft fuel or the maximum number of trials in a computer-based optimization), this factor must necessarily play an important role in the logic of the search procedure. Accordingly, the pdf-guided search algorithm is explicity guided in its internal strategy as a function of the remaining system resources.

This new search technique additionally employs the information gained by previous trials (iterations) in a novel way so as to increase the probability that future trials will yield better performance scores than past trials. The information gained in previous trials is encoded in a multivariate probability distribution function, $p(X|k)$, which denotes the probability that the trial parameter vector $X = (x_1, \ldots, x_N)$ will yield a performance, $P(X)$, which falls within the k^{th} bin in the performance range ($k = 1, \ldots, K$), where $k = 1$ denotes the range of best performance scores. Trial vectors, X, are selected on the basis of yielding good performance. Alternately, trial vectors could be so selected that the probability is low that they will not yield poor performances. A trial vector yielding a poor performance denotes a wasted experiment. Each wasted experiment is costly. Therefore, high penalties are assigned to regions in the parameter space in which trial X vectors are obtained with correspondingly poor performance scores.

After each trial vector X is employed, the performance score, $P(X)$, is noted, and the region of parameter space containing X has a probability assigned to it based on the value of $P(X)$. If $P(X)$ falls within the k^{th} bin, $p(X|k)$ is updated. In this manner, all the information that has been generated since the beginning of the search is encoded in long-term memory PDF's. These, in turn, bias the search away from probable low yield parameter regions and towards probable high yield regions.

The terminology used in referring to the three parts of the PDF search in this report is as follows: PDF1 -- unbiased random sampling (of KTOT points) followed by division of the KTOT points into K performance classes depending upon the associated performance value; PDF2 -- K separate cluster analyses in the N-dimensional space to obtain one multimodal pdf for each of the K classes; PDF3 -- adaptive search phase in which the $p(X|k)$ are updated as outlined above and described in detail in (11, 12, 13).

3.2 Guided Accelerated Random Search (GARS)

The guided accelerated random search (GARS) algorithms are probability-state-variable (psv) searches that are particularly intended for applications involving multimodal performance surfaces. These algorithms are suitable for spaces of low or high dimensionality and for the search of stationary or time-varying surfaces. The more flexible of the GARS algorithms contain the following provisions:

(a) Uniform Random Phase -- A search phase in which a uniform pdf is employed to govern the generation of random trials. The heuristic principals of reversal, acceleration, and deceleration are incorporated for the exploitation of the results of random experimentation.

(b) Biased Search Phase -- A search phase in which the pdf is adjusted in accordance with the results of ongoing trials so as to increase the rate of their convergence. This is the most important of the GARS phases and utilizes three basic methods of governance of random experiments. The principals of reversal, accelerations and decelerations are again employed, as in the uniform random phase, subsequent to each random experiment producing an improved or worsened score.

(c) Biased Random Phase with Activity Factor -- A phase in which the fraction of the total number of free variables subject to manipulation is progressively reduced from unity until approximately two variables only (on the average) are being adjusted. An activity factor, which is a function of trial number and/or performance, determines the a priori probability that a specific parameter will be varied in any given random trial. The identity of parameters manipulated is kept random while the activity factor is systematically reduced. This phase is the same as (b) except for the use of an activity factor.

(d) Systematic Phase -- A phase in which a steepest-descent (or ascent) principal is used (with small activity factor in the case of high-dimensional problems) for the "fine tuning" of performance in the vicinity of best results from a preceding random phase.

(e) Systematic Phase With Single-Dimension Manipulation -- Subsequent to the steepest-descent adjustment, a systematic one dimension-at-a-time adjustment is made of the manipulable parameters.

In addition to the concepts of reversal, acceleration, and deceleration mentioned above and described in the general literature (2, 3, 9), several additional principals are embodied in the general GARS-type algorithms. These relate to the observance of boundaries on the admissible values of parameters, procedures for periodic reinitialization of GARS so that the record of best-to-date-performance does not become misleading if the performance surface is varying with time, and use of certain methods for controlling the directions and lengths of random steps.

All of the probability state variable techniques, including GARS, offer rapid convergence and have the ability to deal with the problem of time-varying surfaces and high levels of noise in measurements.

The method or methods used for storage of performance data are of great importance in advanced versions of self-organizing and learning systems because the efficiency of such systems is highly dependent on the memory processes used. This is particularly true for multivariate systems: if one uses conventional methods, the retention and accession of information become increasingly difficult as the number of variables increases. Accordingly, those procedures suitable for encoding long-term memory for self-organizing and learning systems were investigated.

3.3 Composite Search Technique Combining PDF and GARS Algorithms

Each of the techniques described above has certain advantages and disadvantages. GARS is fast and accurate, but its convergence rate is somewhat dependent on the choice of a starting point. GARS can sometimes spend considerable time extracting itself from local maxima. PDF can more accurately learn the general topography of the performance surface and, consequently, it can distinguish between local and global maxima quite well. Its main disadvantages are that it is slow and it is unlikely to discover the centroid of the global maximum without high expenditure of resources (i.e., large amounts of searching in the immediate vicinity of the global maximum).

A more general and powerful approach would be to combine PDF and GARS. The multimodal statistical capabilities of PDF would be substituted for the unimodal statistical strategy of GARS' random phases. Such a method would not only retain the virtues of each algorithm, but would yield other benefits not possessed by either alone.

To begin with, PDF provides GARS with a good starting point. This can be either the best single point found by PDF or the cluster center of the mode possessing the highest performance value. If there is more than one extremal point of interest, the PDF results can be employed to locate the regions in which they occur, and to initialize a search in each one. The knowledge of the topography of the performance surface acquired by PDF can also be used to more effectively prevent GARS from falling into regions with high resource penalties or low performance score.

Perhaps the most important benefit of combining PDF with GARS is the increased sophistication and efficiency that PDF can give to the second and third phases of GARS (the statistically biased search phases). As GARS is presently formulated, a unimodal pdf is generated, centered at the current best-to-date point, and this distribution is used to choose the next trial point. This method is a considerable improvement over simple random sampling, but it mainly confines the search to a (Gaussianly-shaped) neighborhood of the current best-to-date point. Limiting the search in this way both slows convergence and may result in the search occasionally and unnecessarily becoming stranded on a local maximum for a long period. Substituting the multimodal distribution function adaptively developed by PDF will provide GARS with much more information about the performance surface. This will enable GARS to make better choices of new trial points. The results of each trial can be used adaptively to update the pdf model, leading to more efficient searching.

3.4 Experimental Procedure

The procedure followed in this investigation was a modest first effort at approximating the composite search algorithm described above. It does, however, demonstrate that combining the two techniques is both feasible and desirable.

The experimental procedure was as follows. The test surface was selected to be the performance function described in Section 2. It was first searched (for the global maximum) using the PDF algorithm. This consists of an initial random sampling followed by a clustering analysis, then a pdf-guided search, until the system's resources were exhausted as described above in Section 3.1.

GARS was initialized in three different ways. First, the random phase was deleted and the first biased phase started from the best point found by PDF. Second, the random phase was again deleted and the biased phase started from the center of one of the clusters formed by PDF from the points in the top performance class. These first two schemes for selecting a starting point for GARS, in effect, substituted PDF for the random search phase of GARS. The third technique was to use a cluster center from the lowest performance class as the starting point for GARS. This ensured that the starting point would be far enough from the global maximum to allow for a valid comparison to "better" starting points. In this third case, the initial random search phase was retained.

Table 5 summarizes the 42 experimental searches that were made on the five performance surfaces. NDIM is the dimensionality of the surface; KTOT is the number of samples in the random phase of PDF (note that for NDIM = 2, 5, and 10, there is more than one value of KTOT). Changing the number of random samples affects the structure of the cluster model and the percentage of the initial resources that is consumed. The strategy for the pdf-guided search is therefore altered as well. The GARS starting point is identified in one of five ways:

x^*	-	PDF best point
$\bar{x}$	-	Center of cluster in top performance class (if there are more than one such cluster, they are numbered consecutively, $\bar{x}_1, \bar{x}_2$, etc.)
$\bar{x}_B$	-	Center of cluster in lowest performance class
x_o	-	Origin of space (2 and 20 dimensions only)
x_c	-	A random point (2 dimensions only)

To ensure that $\bar{x}_B$ was not too far from the global maximum to be validly compared to x^* and $\bar{x}$, x_o and x_c were used as checks. The values of all the starting points are listed in Tables 6 through 10 along with the final (best) point and, for each value of NDIM, the location of the global maximum.

3.5 Illustrative Example

The results of the 42 searches are given in Tables A-1 through A-11 of Appendix A. To clarify the experimental procedure and to aid in interpreting results, Run 1 of Table A-1 can serve as an illustration.

TABLE 5

FORTY-TWO SEARCHES MADE WITH COMPOSITE ALGORITHM

Run Number	NDIM	KTOT	GARS Starting Point
1	2	50	x^*
2	2	50	$\bar{x}$
3	2	100	x^*
4	2	100	$\bar{x}$
5	2	200	x^*
6	2	200	$\bar{x}_1$
7	2	200	$\bar{x}_2$
8	2	200	$\bar{x}_3$
9	2	200	$\bar{x}_4$
10	2	-	x_0
11	2	-	x_c
12	2	200	$\bar{x}_B$
13	5	100	x^*
14	5	100	$\bar{x}_1$
15	5	100	$\bar{x}_2$
16	5	200	x^*
17	5	200	$\bar{x}_1$
18	5	200	$\bar{x}_2$
19	5	200	$\bar{x}_3$
20	5	200	$\bar{x}_4$
21	5	200	$\bar{x}_5$
22	5	200	$\bar{x}_6$
23	5	200	$\bar{x}_7$
24	5	200	$\bar{x}_8$
25	5	200	$\bar{x}_B$
26	10	100	x^*
27	10	100	$\bar{x}$
28	10	200	x^*
29	10	200	$\bar{x}_1$
30	10	200	$\bar{x}_2$
31	10	200	$\bar{x}_B$
32	15	200	x^*
33	15	200	$\bar{x}_1$
34	15	200	$\bar{x}_2$
35	15	200	$\bar{x}_3$
36	15	200	$\bar{x}_B$
37	20	200	x^*
38	20	200	$\bar{x}_1$
39	20	200	$\bar{x}_2$
40	20	200	$\bar{x}_3$
41	20	200	$\bar{x}_B$
42	20	200	x_0

TABLE 6

STARTING AND FINAL POINTS FOR SEARCHES OF TWO-DIMENSIONAL TEST FUNCTION

Run Number	Starting Point		Final Point	
1	-.663	-.054	-.670	-.045
2	-.635	-.069	-.675	-.046
3	-.666	-.048	-.667	-.049
4	-.640	.138	-.671	-.048
5	-.690	-.050	-.671	-.045
6	-.682	.391	-.671	-.048
7	-.507	.044	-.675	-.047
8	-.886	.165	-.671	-.046
9	-.708	-.232	-.670	-.046
10	.000	.000	-.670	-.051
11	.570	-.990	-.672	-.048
12	.752	.698	-.672	-.048

True Maximum: -0.671, -0.046

TABLE 7

STARTING AND FINAL POINTS FOR SEARCHES OF FIVE-DIMENSIONAL TEST FUNCTION

Run Number	Starting Point					Final Point				
13	-.698	-.310	-.554	.559	-.619	-.710	-.025	-.190	.745	-.854
14	-.361	.151	-.134	.324	-.123	-.710	-.029	-.188	.746	-.858
15	-.759	.200	.341	.449	.074	-.710	-.028	-.192	.747	-.859
16	-.624	-.126	-.282	.584	-.385	-.713	-.030	-.193	.745	-.855
17	-.518	.236	-.382	.413	.416	-.711	-.024	-.191	.746	-.854
18	-.315	.567	.019	.568	.655	-.711	-.025	-.189	.745	-.854
19	-.383	.363	.526	.139	.123	-.713	-.026	-.191	.745	-.857
20	-.593	-.597	-.249	.414	-.272	-.709	-.026	-.190	.748	-.855
21	-.423	.427	.326	.614	-.351	-.710	-.028	-.188	.746	-.857
22	-.792	.209	-.190	.557	-.430	-.710	-.023	-.188	.749	-.854
23	-.625	.402	-.324	-.239	.337	-.711	-.027	-.191	.746	-.854
24	-.238	.448	.532	-.126	.757	-.818	.466	.004	.191	.610
25	.032	-.957	.694	.630	-.863	-.712	-.023	-.193	.745	-.855

True Maximum: -0.710, -0.025, -0.187, 0.746, -0.855

TABLE 8

STARTING AND FINAL POINTS FOR SEARCHES OF TEN-DIMENSIONAL TEST FUNCTION

Run Number	Starting Point					Final Point				
26	-.406	.426	.114	.897	-.977	-.737	.014	-.237	.755	-.856
	.026	-.434	-.346	.500	-.112	.246	-.786	-.445	.544	-.155
27	-.528	.059	-.072	.217	-.086	-.733	.013	-.236	.756	-.860
	.201	-.091	-.044	.313	-.177	.244	-.789	-.441	.541	-.152
28	-.406	.426	.114	.897	-.977	-.737	.014	-.237	.755	-.856
	.026	-.434	-.346	.500	-.112	.246	-.786	-.445	.544	-.155
29	-.500	.153	-.189	.225	-.037	-.732	.015	-.239	.755	[illegible]
	.238	-.141	-.106	.436	-.106	.246	.790	-.445	.542	-.154
30	-.557	.222	.028	-.431	.384	-.838	.495	.020	.116	[illegible]
	.174	.430	.213	.301	-.044	.705	.580	-.051	.661	.061
31	-.162	-.496	-.396	.514	-.186	-.737	-.014	-.235	.755	-.862
	-.683	-.793	.649	-.305	.643	.241	-.790	-.445	.541	-.151

True Maximum: -0.734, -0.014, -0.237, 0.755, -0.859

0.246, -0.788, -0.442, 0.543, [illegible]

TABLE 9

STARTING AND FINAL POINTS FOR SEARCHES OF 15-DIMENSIONAL TEST FUNCTION

Run Number	Starting Point					Final Point				
32	-.522	.751	.404	.074	.698	-.842	.457	-.065	.395	.647
	.297	.517	-.711	.233	.020	.420	.555	-.540	.702	-.144
	.538	-.850	.555	-.246	-.421	.421	-.455	.938	-.286	-.697
33	-.214	.436	-.090	.121	.247	-.849	.463	-.063	.389	.654
	.065	.260	-.220	.117	-.172	.424	.563	-.539	.705	-.144
	.256	-.167	.323	-.072	-.353	.416	-.441	.940	-.293	-.692
34	-.420	.553	.091	.710	-.384	-.847	.460	-.065	.390	.649
	.158	-.320	-.278	.358	-.481	.421	.559	-.539	.704	-.146
	.069	.002	-.004	-.442	-.640	.422	-.452	.940	-.290	-.695
35	-.519	.211	.469	.215	-.212	-.848	.466	-.062	.389	.655
	.275	.255	.169	.062	-.519	.424	.561	-.533	.707	-.145
	.552	-.685	-.478	-.475	-.736	.420	-.444	.938	-.292	-.692
36	.530	.448	-.104	.528	-.629	-.842	.458	-.066	.393	.647
	-.353	.489	.402	-.855	.873	.420	.559	-.540	.701	-.144
	-.596	.697	.148	-.275	-.686	.422	-.453	.938	-.290	-.695

True Maximum: -0.848, 0.463, -0.063, 0.390, 0.653
0 423, 0.561, -0.537, 0.705, -0.145
0.420 -0.446, 0.939, -0.292, -0.693

TABLE 10

STARTING AND FINAL POINTS FOR SEARCHES OF 20-DIMENSIONAL TEST FUNCTION

Run Number	Starting Point						Final Point					
37	-.151	.984	-.083	.712	.243	.993	-.975	.486	-.055	.743	.663	.380
	.336	-.436	.445	-.450	.272	-.086	.536	-1.000	.831	-.311	.593	-.735
	-.138	-.158	.187	.184	704	-.943	.879	-.180	-.730	-.635	.814	-.821
	-.225	-.374					-.143	-.481				
38	-.091	.345	.139	.239	.249	.052	-.974	.489	-.058	.743	.662	.380
	.291	-.141	.155	-.136	.147	.015	.533	-1.000	.835	-.312	.593	-.729
	043	-.079	-.176	.034	.344	-.146	.377	-.180	-.732	-.638	.814	-.826
	.116	.178					-.141	-.477				
39	-.560	.074	-.865	.630	.899	.031	-.979	.489	-.059	.744	.660	.378
	.581	-.932	-.912	.925	.081	-.430	.535	-1.000	.834	-.308	.591	-.735
	.531	.130	-.517	-.585	.165	.898	.878	-.184	-.735	-.639	.814	-.823
	-.535	-.741					-.146	-.482				
40	-.382	.763	.318	-.903	-.287	-.270	-.975	.486	-.056	.746	.660	.377
	.564	-.933	.830	.852	.267	.874	.535	-1.000	.837	-.310	.596	-.734
	.779	.601	-.595	-.834	.867	-.178	.880	-.180	-.735	-.639	.818	-.820
	-.794	-.855					1.420	-.480				
41	.454	-.493	-.236	-.608	-.291	.418	-.977	.485	-.056	.745	.660	.376
	.193	.250	-.190	.473	.028	-.527	.534	-1.000	.834	-.314	.595	-.734
	.407	.364	-.194	.306	-.228	.562	.379	-.182	.734	-.641	.816	.818
	-.211	-.084					-.141	-.481				
42	0.000	0.000	0.000	0.000	0.000	0.000	-.977	.485	-.059	.745	.660	.376
	0.000	0.000	0.000	0.000	0.000	0.000	.534	-1.000	.834	-.314	.595	-.734
	0.000	0.000	0.000	0.000	0.000	0.000	.879	-.182	-.734	-.641	.816	-.818
	0.000	0.000					-.141	-.481				

True Maximum -0.976, 0.486, -0.056, 0.745, 0.660, 0.377
0.535, -1.000, 0.835, -0.312, 0.595, -0.734
-0.879, -0.181, -0.734, -0.640, 0.817, -0.819
-0.142, -0.481

Run 1 was a combined search on the two-dimensional test surface. The locations, sizes, and amplitudes of the performance function were given above in Tables 1 through 3, and the location and functic value of the global maximum were given in Table 4.

The system initially possessed 400 units of resources, or 200 units per dimension. Fifty random trials were made, equalling 25 per dimension. The system resources are depleted on each trial by the difference between unity and the maximum function value, whichever is larger, and the function value of the trial point. Since the minimum function value is approximately -1, the average function value should be approximately 0, and the penalty per random trial is approximately 1. This is confirmed by the resource consumption in PDF1, the unbiased random search--52.60 units for 50 trials--which constitutes a loss of 13.15 percent of the total syste resources. The best point found by the random search in Run 1 had a function value of 0.9897, or 97.4 percent of the maximum value of 1.0164.

In order to facilitate comparisons between experiments, the distance from the best point to the global maximum has been normalized by the maximum diameter of the hypercubical space. For each of the five test surfaces the space is a hypercube with each dimension taking on values from -1 to +1. Therefore, the maximum distance between the two points is 2 x $(\mathrm{NDIM})^{\frac{1}{2}}$, where NDIM is the dimensionality of the test surface. Thus, for Run 1, the normalized distance from the best to the maximum is 0.02.

PDF2, the second section of PDF, is a clustering analysis. In this case, the 50 sample points fall into 12 clusters.

PDF3 is the guided search phase. In this case, the system resources were not expended until 500 trials (250 trials per dimension) had occurred. This is a strong indication that the search is focusing increasingly on the higher performance class as it should, as explained above in Section 3.2. The 500 trials consumed only

347.40 resource units, or 0.70 units per trial. This is substantially lower than the average of 1.05 units per trial in PDF1, indicating that the average performance is considerably higher. The resource consumed in PDF3 was 86.85 percent of the initial system resource, that is, all that remained upon terminating PDF1.

The best point found by PDF3 has a function value of 1.0155, which is 99.9 percent of the maximum value. The point itself is a negligible distance from the global maximum. The difference in function values between the PDF3 best point and the PDF1 best point is 0.0258.

The GARS search in Run 1 is begun with the best point from the PDF search as shown in Tables 6 through 10. Part 1, the random search, is deleted since PDF has already fulfilled the purpose. Parts 2 and 3 of GARS, the biased search phases, are allowed to run for a maximum of 50 iterations each. Neither part can improve on the starting point. (At the current stage in the development of GARS, Parts 2 and 3 employ a unimodal pdf, centered at the current best point, to choose the next trial point. The multimodal distribution generated by the PDF algorithm has not yet been incorporated as discussed in Section 3.3.) The gradient search phase, Part 4, is also allowed 50 iterations; it succeeds once in finding a better point. The function value of the point is 1.0158 or 99.9 percent of the function maximum. The normalized distance from the new best point to the global maximum is 0.03. (Note that it is possible for a point farther from the global maximum to have a higher function value than another, closer point.) The fine-tuning phase of GARS, Part 5, is allowed only 20 iterations; it improves on the best poi t once. The new best point has a function value of 1.0164, the maximum function value, and is at a near-zero normalized distance from the global maximum.

Overall in Run 1, then, GARS was allowed to make 170 iterations and had two successes. The best point, its percentage of the maximum value and its distance from the global maximum, are as given for Part 5. The improvement of the GARS highest function value over the PDF highest function value is 0.0009.

3.6 Results and Conclusions

Tables A-1 through A-11 list results by run; Figures 1 through 3 present the most significant overall results of the investigation.

Figure 1 shows the percent of maximum function value achieved by PDF as a function of the estimated number of trials per dimension. The estimated number of trials for a given experiment is the number of trials the system can be expected to make before running out of resources. It is computed by dividing the amount of initial system recource by the estimated average resource consumption per trial. In this problem, the values of the performance function ranged from -1 to +1, and the estimated average resource consumption is one unit per trial. Then in the case where the initial system resource is 400, the estimated number of trials is 400; if the dimensionality is 2, the estimated number of trials per dimension is 200.

Figure 1 also illustrates the rate at which the global maximum is reached with respect to the number of trials per dimension a search is allowed to make. It can be seen that given enough resources to take approximately 200 samples per dimension, PDF can converge to the global maximum. This is not practical for problems of high dimensionality; GARS or a similar technique is needed to supplement PDF for these higher dimensional surfaces.

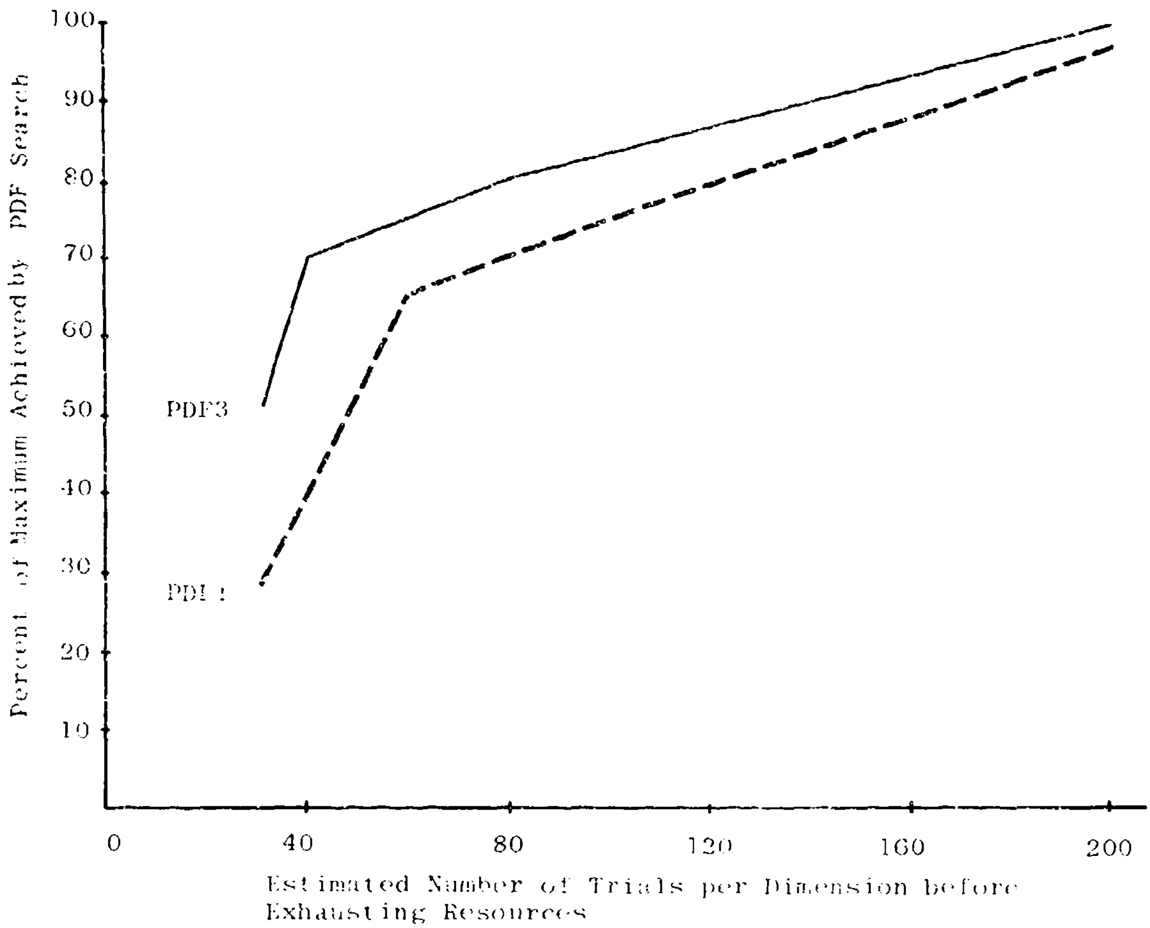

FIGURE 1: EFFICIENCY OF PDF SEARCH

Figures 2 and 3 indicate the influence of PDF on GARS.[1/] Figure 2 illustrates the number of successful moves per dimension (starting from the PDF best point) that GARS requires to achieve the maximum function value, as a function of the estimated number of trials per dimension in PDF1. More time spent in PDF improves the performance surface model and thus enables GARS to operate more efficiently. GARS would be even more effective if it were modified to take fuller advantage of the PDF model.

Figure 3 shows clearly that GARS in combination with PDF is more powerful than GARS alone. For each of the five performance surfaces, the number of successful moves per dimension for GARS to achieve the maximum is given as a function of dimensionality for each of three starting points: x^*, the PDF best point; $\overline{x}$, the cluster center of the best performance class; and $\overline{x}_B$, the cluster center from the low performance class used as an independent starting point. In the cases where there was more than one cluster in the top performance class, the number of moves plotted is the average number of moves for all runs which reached the maximum (see Table 5). Except for one case ($N = 15$ for $x = \overline{x}_B$), GARS reached the maximum more quickly from $\overline{x}$ than from $\overline{x}_B$, and most quickly from x^*. (The minimum at $N = 10$ is probably a function of the particular test surface used.) In the case of $x = \overline{x}_B$ for $N=15$, the GARS random search quickly found a point with a function value almost as large as those cases using the PDF-generated x^* and $\overline{x}$ as starting points. This point was located in a more favorable position on the surface so that GARS spent less time on the biased searches and the gradient search. It is readily apparent that PDF is a valuable preliminary step to GARS, and can profitably be substituted for the random search phase of GARS.

[1/] In Figure 2, the value for the ten-dimensional problem has been set off separately and not been included in the interpolations. The ten-dimensional search discovered its best point in the first, smallest (100-point) random sampling in PDF. It did not improve on this value in a subsequent 200-point random search or in the guided searches following the random searches. Thus the PDF results, the GARS starting points, and the GARS performance are not comparable to those for the other problems.

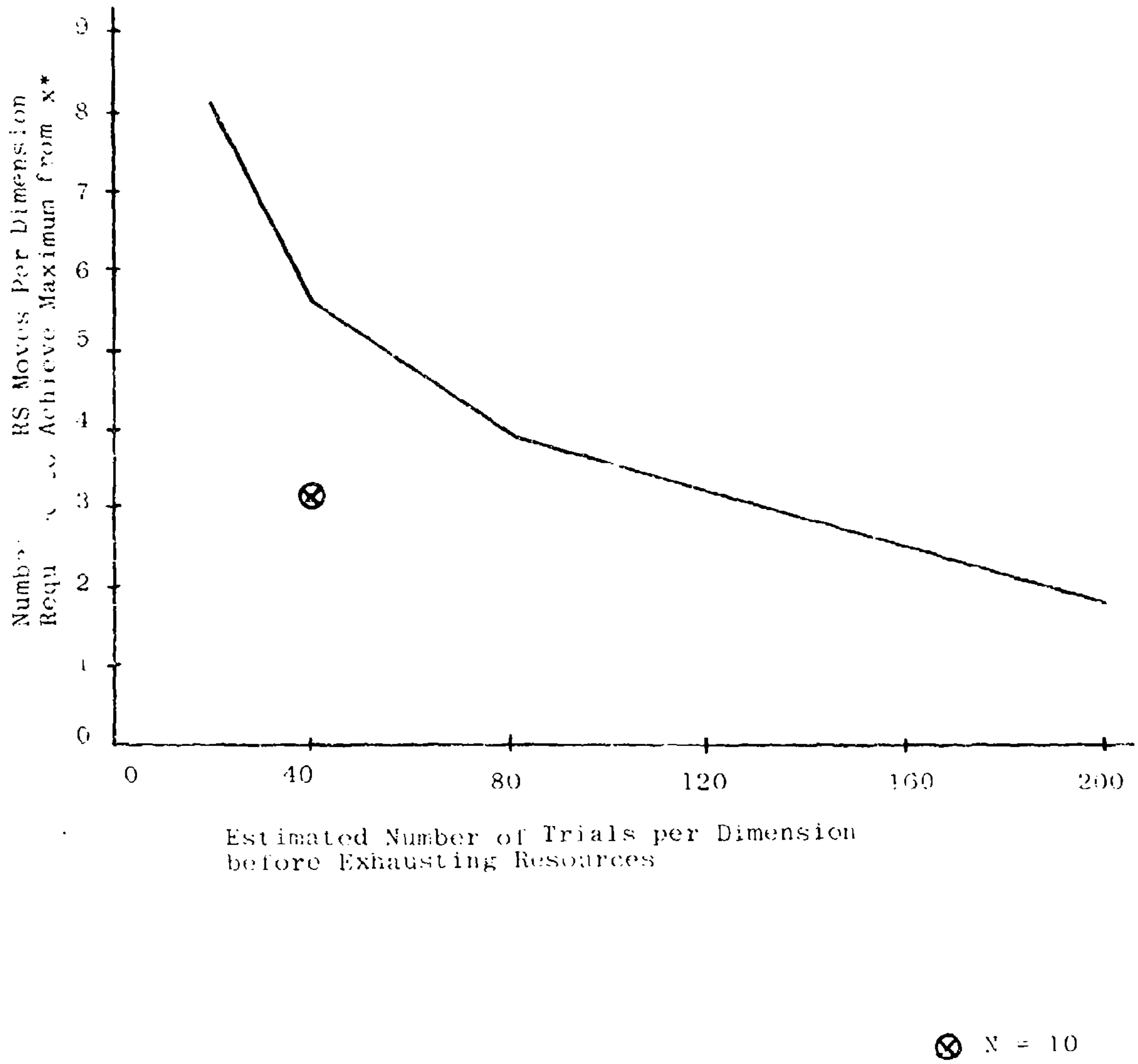

FIGURE 2: EFFICIENCY OF GARS SEARCH

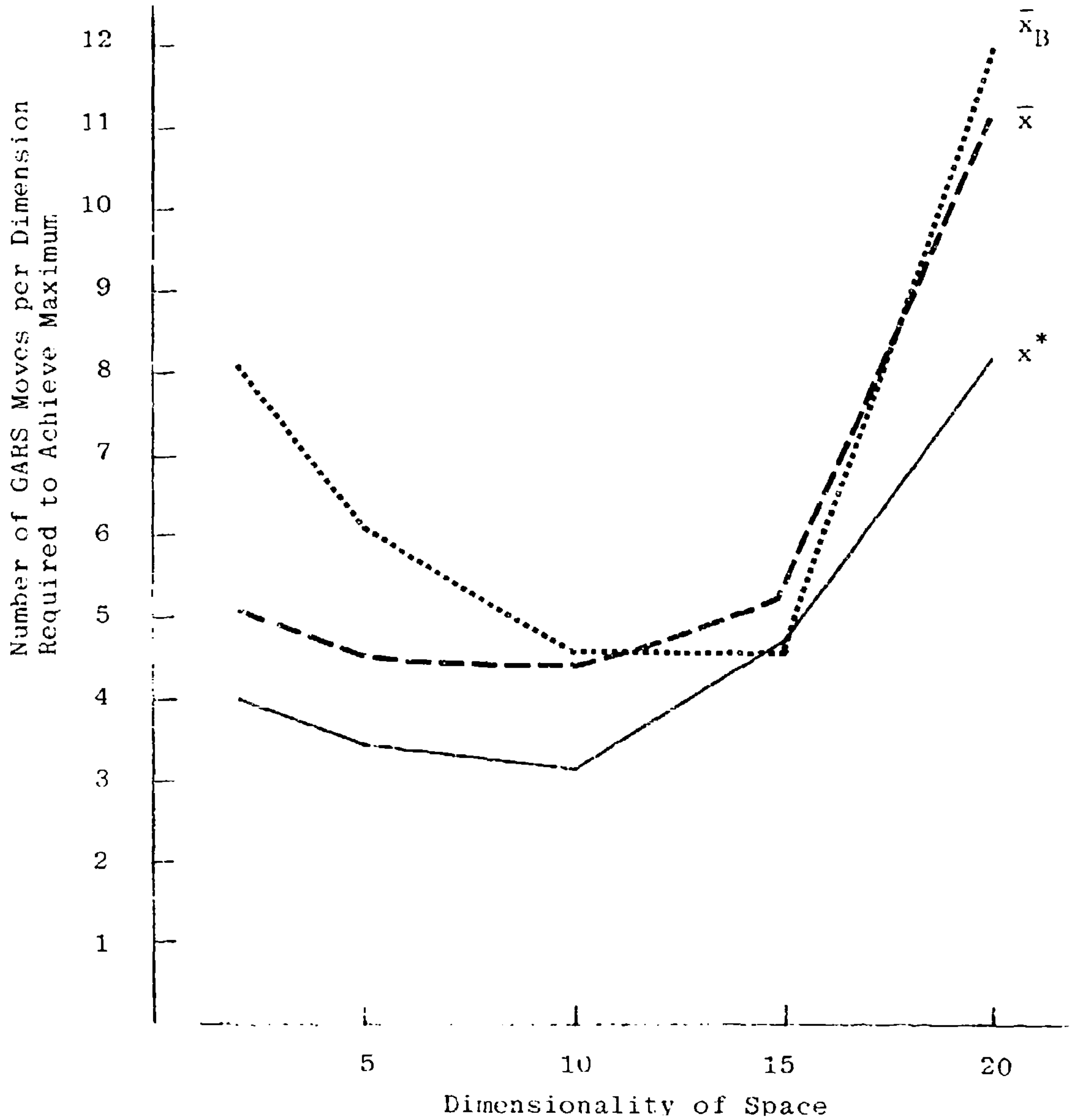

x^* = PDF Best Point as Starting Point

$\bar{x}$ = Center of Cluster in Top Performance Class as Starting Point

$\bar{x}_B$ = Center of Cluster in Lowest Performance Class as Starting Point

FIGURE 3: EFFICIENCY OF PDF-GARS COMPOSITE SEARCH

PDF enables GARS to find not only the global maximum, but other maxima in the high performance class. The ability to locate local maxima can be significant for certain problems. For instance, it may be desirable that a system be able to operate in more than one region in its parameter space. In other cases, operating at or near the global maximum may be unfeasible if this value is close to a catastrophic operating region. (See Run 24, Table A-6 and Run 30, Table A-8.)

SECTION IV

ASSESSMENT OF THE COMPLEXITY OF A SEARCH (OPTIMIZATION) PROBLEM

4.1 Need for a Measure of Complexity

A major problem is to estimate the "complexity" of a search problem. Complexity of the performance hypersurface can be defined to be (1) the number of modes (peaks), (2) their locations relative to each other, (3) their shape and volume, and (4) the estimated maximum performance value within each. If this information were obtainable before beginning a search problem, these data would not only specify the complexity of the search problem, but would also probably identify the most appropriate search strategy.

4.2 Applicability of Cluster Analysis

It was shown in the previous effort (11, 12, 13) that a clustering algorithm can be useful in pointing out regions of a performance surface that have significant locations, volumes, or performance values. It can locate both peaks (maxima) and valleys (minima), and give information concerning the size, location, and approximate extreme value of each.

The procedure to be followed is very similar to Parts 1 and 2 of PDF: a random search followed by a clustering analysis[1/] (see Section 3.4). The performance space should be sampled extensively enough to ensure that no large regions are neglected; that is, the space must be sampled fairly evenly, with no large unsampled gaps, to minimize the possibility of missing a potentially significant extremum.

Following the random search, the sample points are divided into performance classes according to their associated function values. The classes need not have equal function value ranges (i.e., the

---

[1/] The Mucciardi-Gose CLUSTR algorithm was used (10).

difference between upper and lower bounds), or contain equal numbers of sample points. The number of classes is limited only by the number of sample points; that is, there should be a sufficient number of points in each class to make a clustering analysis useful.

Each performance class is clustered separately. The following information is determined: number of cells in each class, location (i.e. center or mean) of each cell, size of each cell, number of points in each cell, and a list of the identity of each point in each cell. In addition, an optional "intercell analysis" may be performed. This analysis locates and identifies pairs of cells which overlap, whether they are in the same class or in different classes. For a given pair, the intercell analysis also estimates the percentage of each cell's volume falling within their common region.

4.3 Illustrative Example

A sample problem is the clearest way of illustrating the utility of clustering analyses as a means of assessing complexity.

The two-dimensional performance surface employed in this study was described in Tables 1 through 4. The locations, shapes, and sizes of the five performance modes are illustrated in Figure 4.

The small ellipse for each mode is located at one "size factor" distance from the center of the mode--the large ellipse at twice that distance. The performance surface consists of three modes of positive height (3, 4, and 5) at the left of the surface, and two modes of negative height (1 and 2) at the right of the surface; that is, three peaks and two valleys. There is a moderate amount of influence between Modes 1 and 4, and 2 and 3; strong influence between Modes 3 and 5, and 4 and 5; and very little influence between any other pairs.

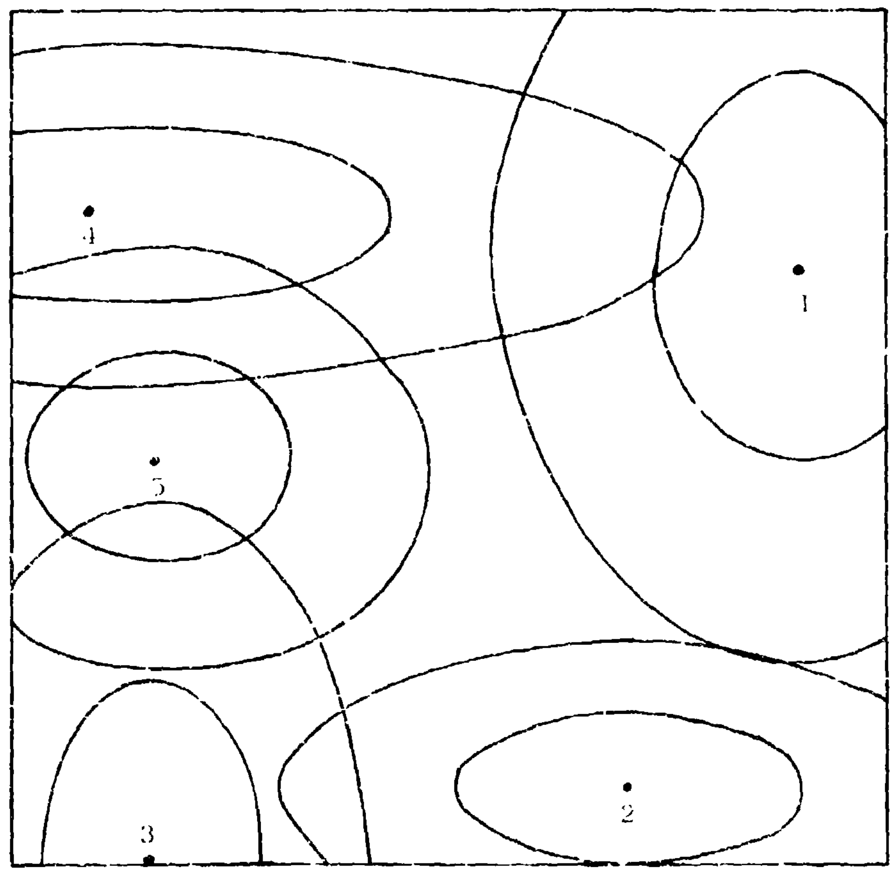

FIGURE 4: TWO-DIMENSIONAL LOCATIONS AND SHAPES OF THE FIVE MODES OF THE PERFORMANCE TEST FUNCTION

For this problem, the four performance classes are divided as follows:

Class 1	-	$0.5 < P$
Class 2	-	$0.0 < P \leq 0.5$
Class 3	-	$-0.5 < P \leq 0.0$
Class 4	-	$P \leq -0.5$

Given the amplitudes of the five modes (as listed in Table 3), we should expect the clustering analysis to construct one or more clusters, close together, in each of the two extreme classes and several distributed over a wider area in each of the two middle classes. A middle-class cluster represents one of two possibilities: a performance mode with its extreme value in the performance class in question, or a region of transition between a higher class and a lower class. The intercell analysis described in Section 4.2 above is useful in determining what a given cell represents. In the first case--a mode with its extreme value in the class in question--the cell will overlap primarily with cells of the next lower class if it contains a peak, or of the next higher class if it contains a valley. In the second case--a transitional region between a higner and a lower class--the cell will overlap with cells from both classes, and possibly with other cells from its own class.

The cluster analysis was performed first on 50 points taken randomly from the surface as shown. It produced 12 clusters, distributed as follows:

Class 1	-	One cluster
Class 2	-	Five clusters
Class 3	-	Five clusters
Class 4	-	One cluster

The locations, shapes and sizes of the clusters are illustrated in Figure 5. Notice that the surface has been incompletely sampled; some of the outer portions of the surface are not included in any of the clusters.

However, even given the sketchiness of the sample, the cluster analysis gives very significant results. Cell 1, the single cluster in Class 1, contains the global maximum; by its position and size it also indicates that the mutual influence of Modes 4 and 5 has broadened the area of performance of Class 1. Cells 2 through 4 describe the region resulting from Mode 4 and the waning influence of Mode 5. Cells 5 and 6 are limited to one point each due to the limited sampling in that region, but they indicate the Class 2 region resulting from Mode 3 and some slight influence of Mode 5.

Cells 7 and 8 cover some of the transitional area between the positive Modes 3 through 5, and the negative Modes 1 and 2. Cell 9 includes not only a good deal of transitional area, but also most of the region dominated by Mode 2. Cell 10 contains only one point, but that point, since it is located on the outer boundary of Cell 12 (the only cell in Class 4), helps to define the limits of Class 4. Cell 11 also contains a single point; it helps to determine the boundary between Class 2 and Class 3.

Cell 12 contains the center of Mode 1; its shift downward is due to the influence of Modes 2 (negative) and 4 (positive). It is noticeably larger than Cell 1 since Mode 1 is larger than Mode 5.

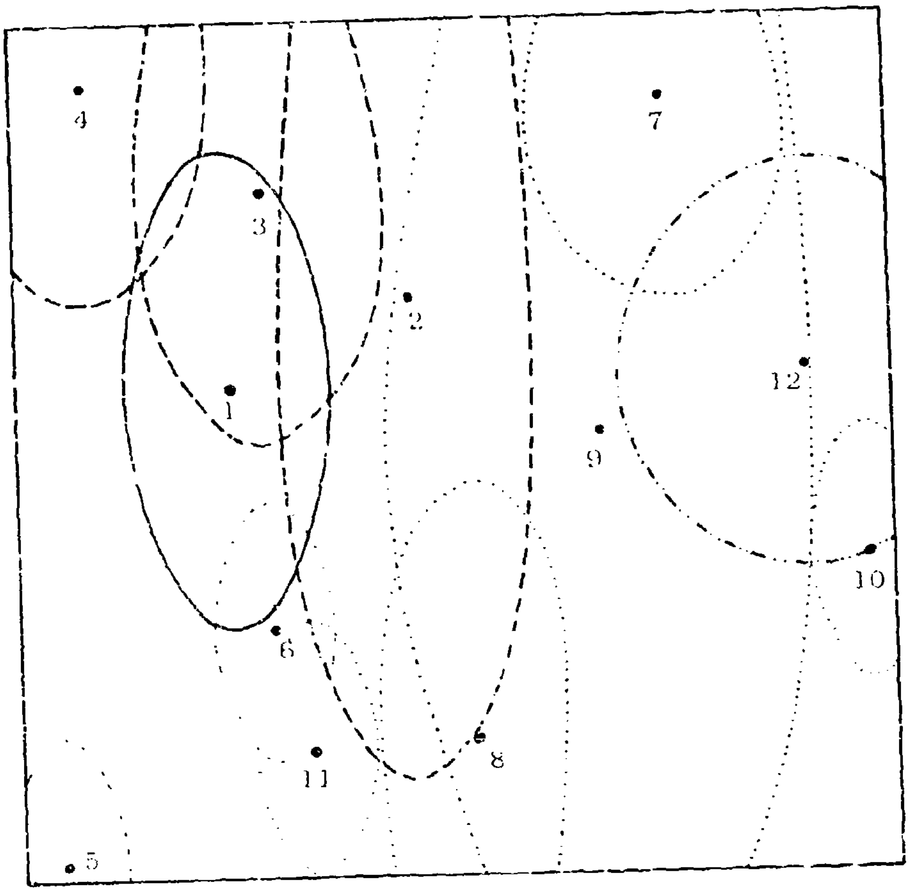

————	Class 1 (Cluster 1)
- - - -	Class 2 (Clusters 2-6)
. . . . .	Class 3 (Clusters 7-11)
-. .-	Class 4 (Cluster 12)

FIGURE 5: CLUSTERING ANALYSIS OF THE TWO-DIMENSIONAL PERFORMANCE TEST FUNCTION (FROM A 50-POINT SAMPLE)

In these examples, the modes in the middle performance classes (Classes 2 and 3) were not isolated. To find them it would only be necessary to increase the random sampling and to make the performance class values narrower. Eventually, each peak would be represented by a cell containing the local maximum, surrounded by rings of cells from decreasing performance classes. Similarly, each valley would produce a cell containing the local minimum, surrounded by rings of cells of increasing performance classes.

The function value of the cell centers in Classes 1 and 4 would give fair approximations of the global maximum and minimum.

A second cluster analysis was performed, this time on a 100-point random sample of the same surface. The results are shown in Figure 6. Due to the increased density of the search, the model defines the boundaries of the four classes more precisely. It is easier to perceive the transition from Class 1 through Classes 2 and 3 to Class 4. In addition, it is clearer that the cell in each extreme class is actually surrounded by a ring of cells in the next lower class (the Class 1 cell surrounded by Class 2 cells) or the next higher class (the Class 4 cell surrounded by Class 3 cells).

In tests run on problems of higher dimensionality, it becomes somewhat more difficult to interpret the results. However, it is evident that cluster analyses, when properly interpreted, are able to provide excellent information concerning the complexity of high-dimensional surfaces. This can be seen from the fact that a clustering analysis of any random sampling of one of the surfaces employed in this project always yielded at least one cell which contained the global maximum. In addition, the number of cells in any class was equal to (and in most cases greater than) the number of performance modes in that class, with two exceptions, as shown in Table 11.

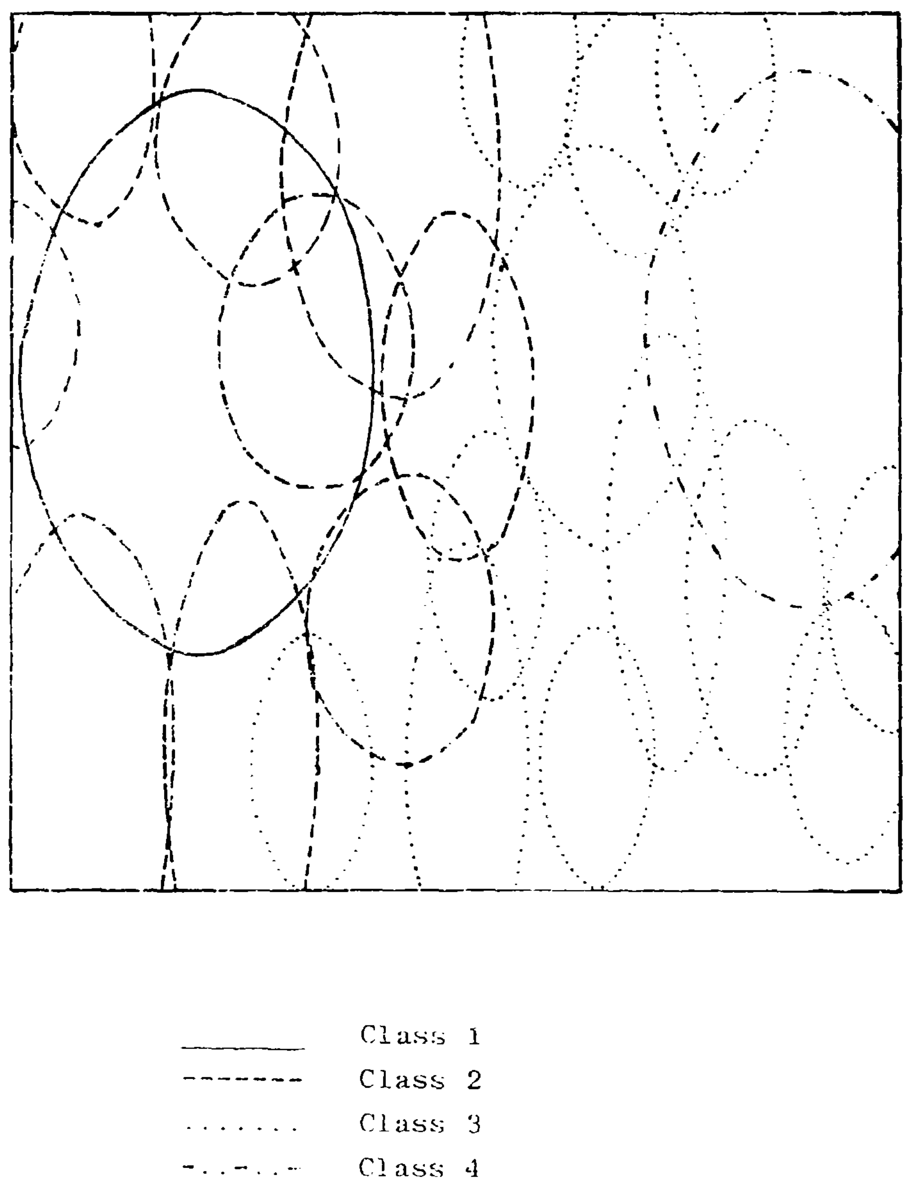

FIGURE 6: CLUSTERING ANALYSIS OF THE TWO-DIMENSIONAL PERFORMANCE TEST FUNCTION (FROM A 100-POINT SAMPLE)

TABLE 11

COMPLEXITY OF PERFORMANCE SURFACE
ESTIMATED BY CLUSTER ANALYSIS

N	KTOT[1/]	Modes In Class				Cells In Class			
		1	2	3	4	1	2	3	4
2	50	1	2	1	1	1	5	5	1
2	100	1	2	1	1	1	9	12	1
2	200	1	2	1	1	4	15	24	5
5	100	2	1	0	2	2	11	7	3
5	200	2	1	0	2	8	24	12	5
10	100	3	0	0	2	1	4	3	6
10	200	3	0	0	2	2	3	6	12
15	200	3	0	0	2	3	13	6	9
20	200	3	0	0	2	3	15	6	8

[1/] Number of Points in Random Sample.

The two exceptions are for Class 1 in the two 10-dimensional searches. In the 10-dimensional problem, the three high performance modes are usually close in dimensions 6, 9 and 10; Modes 3 and 4 are close in dimension 7, and 4 and 5 in 8. (See Table 1). Their strong mutual influence results in a large region of high performance, which is interpreted by the clustering algorithm, as a single cell (in the first case) or as two overlapping cells (in the second).

4.4 Conclusions

It can be seen that clustering analysis fulfills the needs of a complexity assessment: it can discover peaks and valleys, report their locations, estimate their sizes and volumes, provide information for search initiation, and approximate function values. In addition, it can locate and characterize transitional regions. Therefore, the clustering algorithm does provide readily accessible information about the structure of a given performance space.

SECTION V

EXAMINATION OF AN IMAGE-PROCESSING PROBLEM WITH POTENTIAL RPV APPLICATION

One persistent problem in both communication and weapons systems development has been the efficient encoding and transmittal of digitized images. The technique most widely used at present is as follows: Each line of a digitized image is treated as a waveform, the waveform is encoded by performing a Fourier transform. The resulting set of Fourier coefficients for that line is then transmitted, and the picture is reconstructed line-by-line via an inverse Fourier transform.

The set of Fourier coefficients contains as many elements as does the line of data itself (that is, the Fourier transform of a 100-element line has 100 coefficients). It has been found that it is possible to discard some of the coefficients associated with the highest frequencies and transmit the remaining fraction (1, 4, 5, 6, 7). A problem arises in deciding how many coefficients to retain. Of course, fewer coefficients retained and transmitted implies faster and easier transmission and reconstruction. The penalty lies in poorer image resolution.

Since the area of fast Fourier transform (FFT) retention and reconstruction has been thoroughly explored, it seemed beneficial to approach the basic problem -- high accuracy of reconstruction with minimal data transmission -- in an entirely new manner.

Instead of viewing the digitized image a line-at-a-time, the image can be considered as a matrix with each point (element) possessing three descriptors: row, column, and gray level information (e.g., reflectivity, visual density, etc.). Approaching it in this way enables one to visualize the image as a three-dimensional performance surface. That is, gray level information (y) can be regarded as a function of location (row, x_1, and column, x_2).

This approach has three main advantages over the row-by-row approach. First, the eye does not perceive an image in horizontal bands, but as a whole; an encoding technique that does the same can potentially achieve improved subjective information content. Second, by treating a continuous area, an algorithm will be more sensitive to interesting features (e.g., large patches of one gray level, or a repetitive pattern) than a row-by-row analysis can be. Third, identification of regions (i.e., "clusters") of a given gray level in the image also provide the first stage in recognizing classes of objects, or "targets" in the camera's visual field.

The problem of image encoding resembles more closely the problem of assessing complexity (Section 4 -- locating and describing all extrema) than it does the problem of optimization (Section 3 -- locating a single extremum). Therefore, clustering analysis appeared to be quite useful.

5.1 Description of Problem

The problem considered in this portion of the project was the encoding and reconstruction of a photograph of downtown St. Louis, shown in Figure 7. The picture contains very light areas -- the sunlight reflecting from the metal arch -- and very dark areas -- shadows of buildings. It is a rather detailed and complex picture, particularly because areas of common gray level are not always contiguous.

The figure was digitized by division into 32 rows and 32 columns. or 1,024 separate locations. Two hundred and fifty-six levels of gray were used for each of the 1,024 locations. The 2^8 gray levels were condensed into five bands from 1 (black) to 5 (white). The bands were approximately logarithmically chosen as recommended in reference (8):

Gray Level Range	Reduced Range
0 - 34	1 (black)
35 - 79	2
80 - 138	3
139 - 215	4
216 - 255	5 (white)

FIGURE 7: TEST PROBLEM - ORIGINAL PHOTOGRAPH OF DOWNTOWN ST. LOUIS, MISSOURI

A scheme for printing out the digitized picture by computer was devised as recommended in reference (8). The computer reconstruction is shown in Figure 8.

The digitized image was encoded and reconstructed in two ways. First, each class was clustered individually and the picture was reconstructed by assigning each point in the 32 x 32 location matrix to the cell nearest to it. Second, and independently, the picture was subjected to a row-by-row Fourier transform and reconstructed several times, varying the number of coefficients retained.

5.2 Clustering Results

A clustering analysis was performed separately on each performance class in the following manner.

The following number of cells was generated for each class:

Class 1 (black)	-	17
Class 2	-	21
Class 3	-	17
Class 4	-	99
Class 5 (white)	-	9
		163

Figures 9 through 13 show the locations of the various cells in each performance class.

The picture was reconstructed from the 163 clusters in the following arbitrary way; Each point was examined separately; the nearest cell was found and the point was assigned to the performance class associated with that cell.

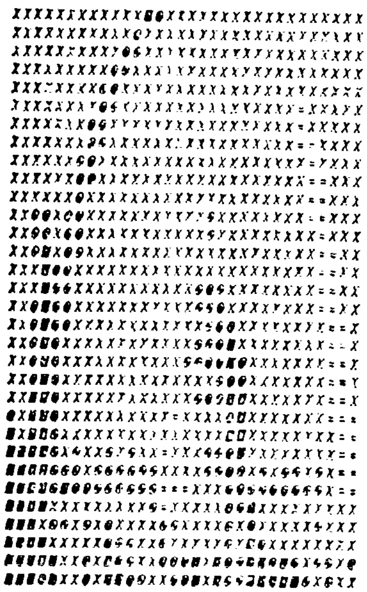

FIGURE 8: COMPUTER REPRESENTATION OF IMAGE IN FIGURE 7

4	4	4	4	4	4	4	4	4	4	4	4	1	2	4	4	4	4	4	4	4	4	4	4	4	4	4	4	4	4	4	4
4	4	4	4	4	4	4	4	4	4	4	2	4	4	4	4	4	4	4	4	4	4	4	4	4	4	4	4	4	4	4	4
4	4	4	4	4	4	4	4	4	4	2	3	4	4	4	4	4	4	4	4	4	4	4	4	4	4	4	4	4	4	4	4
4	4	4	4	4	4	4	4	4	2	2	4	4	4	4	4	4	4	4	4	4	4	4	4	4	4	4	4	4	4	4	4
4	4	4	4	4	4	4	4	3	2	4	4	4	4	4	4	4	4	4	4	4	4	4	4	4	4	4	4	4	4	4	4
4	4	4	4	4	4	4	4	2	3	4	4	4	4	4	4	4	4	4	4	4	4	4	4	4	4	5	4	4	4	4	4
4	4	4	4	4	4	4	2	2	4	4	4	4	4	4	4	4	4	4	4	4	4	4	4	4	4	5	4	4	4	4	4
4	4	4	4	4	4	4	2	3	4	4	4	4	4	4	4	4	4	4	4	4	4	4	4	4	4	5	5	4	4	4	4
4	4	4	4	4	4	3	2	4	4	4	4	4	4	4	4	4	4	4	4	4	4	4	4	4	4	4	5	4	4	4	4
4	4	4	4	4	4	2	2	4	4	4	4	4	4	4	4	4	4	4	4	4	4	4	4	4	4	4	5	5	4	4	4
4	4	4	4	4	4	2	4	4	4	4	4	4	4	4	4	4	4	4	4	4	4	4	4	4	4	4	5	5	4	4	4
4	4	3	2	4	2	2	4	4	4	4	4	4	4	4	4	4	4	3	4	4	4	4	4	4	4	4	5	5	4	4	4
4	4	3	2	4	2	2	4	4	4	4	4	4	4	4	4	4	4	3	4	4	4	4	4	4	4	4	4	5	4	4	4
4	4	3	1	4	2	3	4	4	4	4	4	4	4	4	4	4	4	4	4	4	4	4	4	4	4	4	4	5	5	4	4
4	4	4	1	2	2	4	4	4	4	4	4	4	4	4	4	4	4	4	4	4	4	4	4	4	4	4	4	5	5	4	4
4	4	4	1	2	2	4	4	4	4	4	4	4	4	4	4	4	3	2	3	4	4	4	4	4	4	4	4	5	5	4	4
4	4	2	1	2	2	4	4	4	4	4	4	4	4	4	4	4	3	3	2	4	4	4	4	4	4	4	4	5	5	4	4
4	4	2	1	2	2	4	4	4	4	4	4	4	4	4	4	4	4	3	2	2	4	4	4	4	4	4	4	4	5	5	4
4	4	3	1	2	4	4	4	4	4	4	4	4	4	4	4	4	3	3	2	1	4	4	4	4	4	4	4	4	5	5	4
4	4	2	1	2	4	4	4	4	4	4	4	4	4	4	4	3	3	2	2	1	2	4	4	4	4	4	4	4	5	5	4
4	4	2	1	2	4	4	4	4	4	4	4	4	4	4	4	4	4	4	3	2	2	4	4	4	4	4	4	4	5	5	4
4	4	1	1	2	4	4	4	4	4	4	4	4	4	4	4	4	3	2	2	1	1	4	4	4	4	4	4	4	5	5	4
2	4	1	1	2	4	4	4	4	4	4	4	4	4	4	5	4	4	4	4	2	1	4	4	4	4	4	4	4	5	5	5
1	4	1	1	3	4	4	4	4	4	4	4	4	4	4	4	4	4	4	4	1	1	4	4	4	4	4	4	4	4	5	5
1	1	1	1	3	4	3	4	4	3	4	3	4	4	5	4	4	4	3	4	2	1	4	4	4	4	4	4	4	4	5	5
1	1	1	1	3	3	3	4	3	3	3	3	3	3	4	4	4	4	3	3	2	2	4	3	4	3	3	4	3	4	5	5
1	1	1	1	3	1	2	2	3	3	3	3	3	3	5	5	5	4	4	4	2	2	3	3	2	2	2	3	3	4	5	5
1	1	1	1	4	4	4	4	4	4	4	4	4	3	5	4	4	4	4	4	2	2	1	4	4	4	4	4	4	4	4	4
2	1	1	4	3	3	4	3	4	2	4	4	4	4	3	3	4	4	4	4	3	4	2	4	4	4	4	4	3	4	4	4
1	1	1	1	4	4	4	4	4	2	3	3	4	4	3	4	4	4	4	4	3	4	1	2	4	4	4	4	4	4	4	4
1	1	1	1	1	4	4	2	4	1	2	3	4	4	2	2	2	1	4	1	2	3	1	1	2	1	2	4	3	3	4	2
1	1	1	2	1	4	4	2	4	1	1	2	3	4	4	2	2	1	4	1	3	3	1	1	1	1	1	3	4	3	4	4

FIGURE 9: CLUSTER STRUCTURE OF GRAYNESS CLASS NO. 1

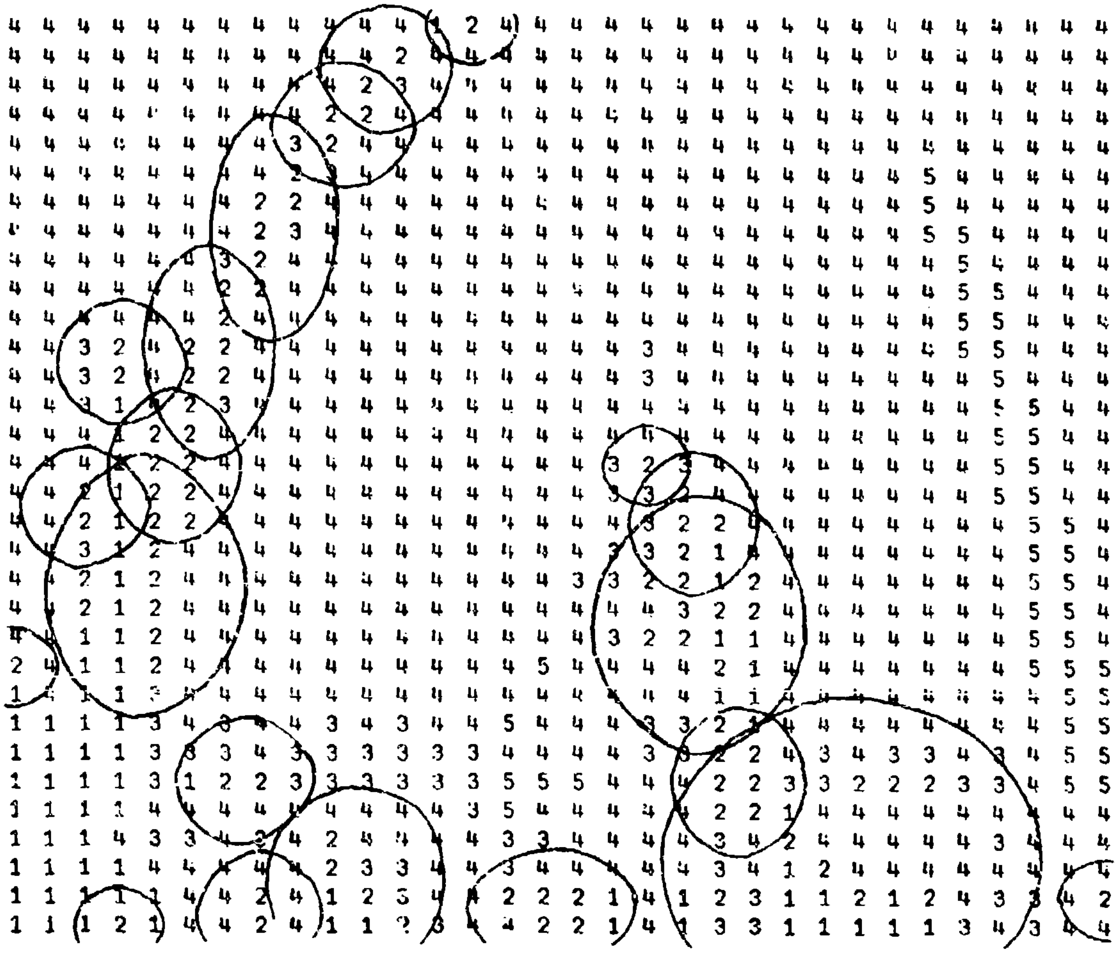

FIGURE 10: CLUSTER STRUCTURE OF GRAYNESS CLASS NO. 2

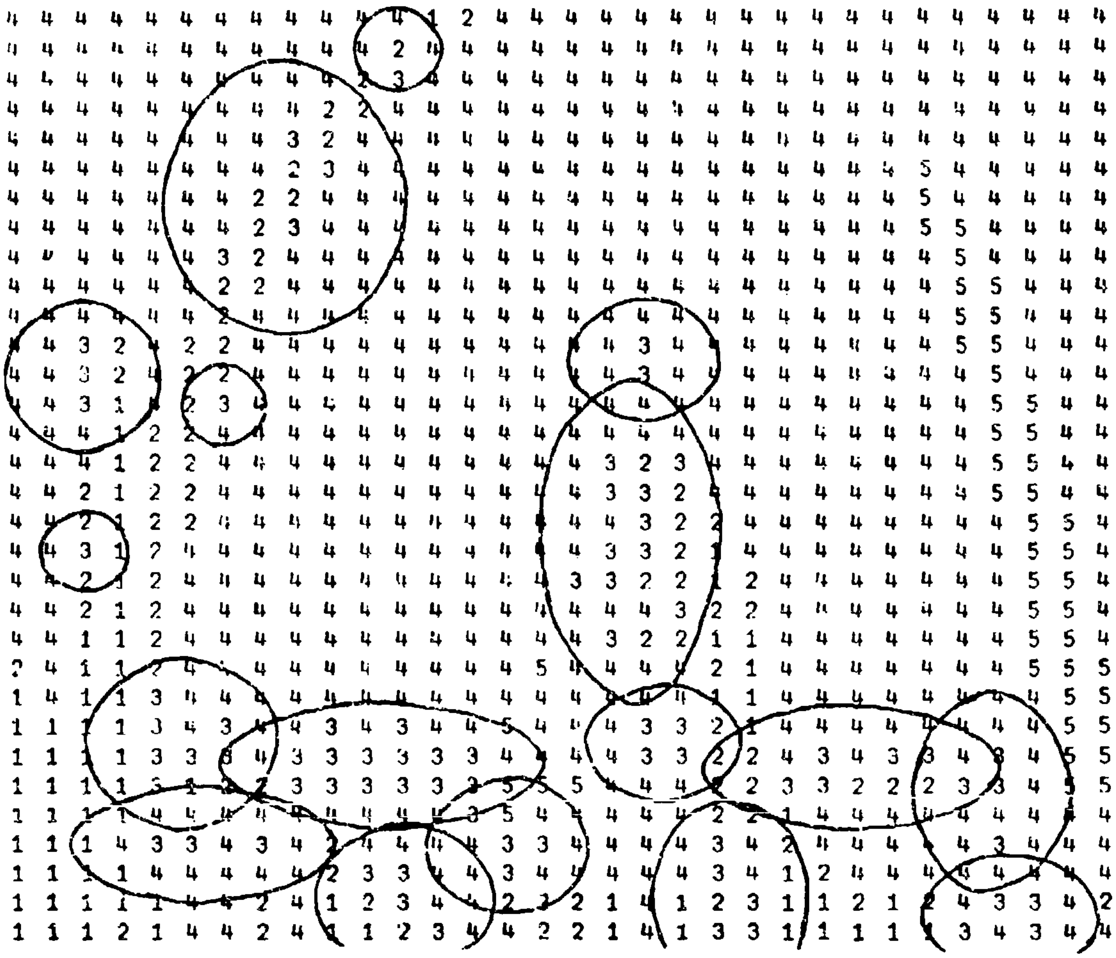

FIGURE 11: CLUSTER STRUCTURE OF GRAYNESS CLASS NO. 3

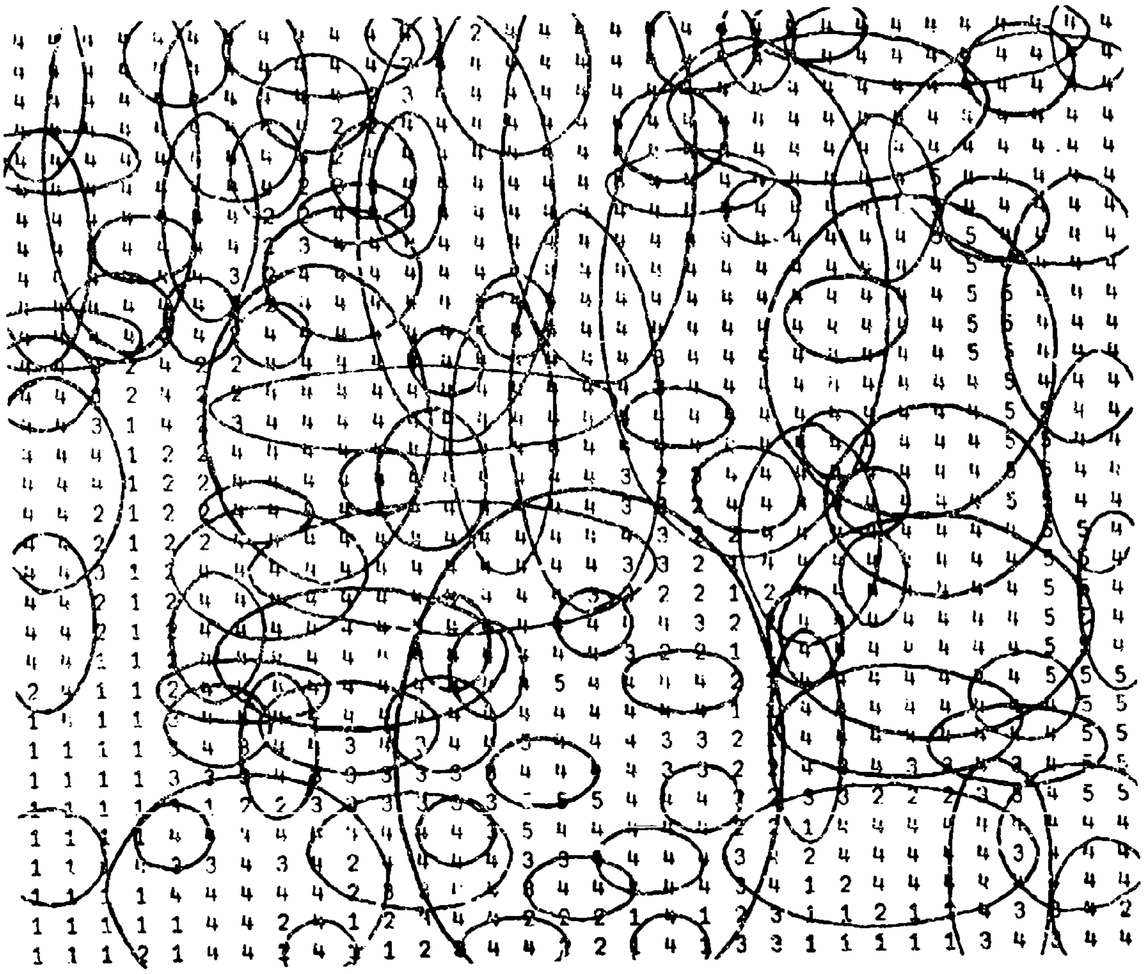

FIGURE 12: CLUSTER STRUCTURE OF GRAYNESS CLASS NO. 4

4	4	4	4	4	4	4	4	4	4	4	4	1	2	4	4	4	4	4	4	4	4	4	4	4	4	4	4	4	4	4	4
4	4	4	4	4	4	4	4	4	4	4	2	4	4	4	4	4	4	4	4	4	4	4	4	4	4	4	4	4	4	4	4
4	4	4	4	4	4	4	4	4	4	2	3	4	4	4	4	4	4	4	4	4	4	4	4	4	4	4	4	4	4	4	4
4	4	4	4	4	4	4	4	4	2	2	4	4	4	4	4	4	4	4	4	4	4	4	4	4	4	4	4	4	4	4	4
4	4	4	4	4	4	4	4	3	2	4	4	4	4	4	4	4	4	4	4	4	4	4	4	4	4	4	4	4	4	4	4
4	4	4	4	4	4	4	4	2	3	4	4	4	4	4	4	4	4	4	4	4	4	4	4	4	4	5	4	4	4	4	4
4	4	4	4	4	4	4	2	2	4	4	4	4	4	4	4	4	4	4	4	4	4	4	4	4	4	5	4	4	4	4	4
4	4	4	4	4	4	4	2	3	4	4	4	4	4	4	4	4	4	4	4	4	4	4	4	4	4	5	5	4	4	4	4
4	4	4	4	4	4	3	2	4	4	4	4	4	4	4	4	4	4	4	4	4	4	4	4	4	4	4	5	4	4	4	4
4	4	4	4	4	4	2	2	4	4	4	4	4	4	4	4	4	4	4	4	4	4	4	4	4	4	4	5	5	4	4	4
4	4	4	4	4	4	2	4	4	4	4	4	4	4	4	4	4	4	4	4	4	4	4	4	4	4	4	5	5	4	4	4
4	4	3	2	4	2	2	4	4	4	4	4	4	4	4	4	4	4	3	4	4	4	4	4	4	4	4	5	5	4	4	4
4	4	3	2	4	2	2	4	4	4	4	4	4	4	4	4	4	4	3	4	4	4	4	4	4	4	4	4	5	4	4	4
4	4	3	1	4	2	3	4	4	4	4	4	4	4	4	4	4	4	4	4	4	4	4	4	4	4	4	4	5	5	4	4
4	4	4	1	2	2	4	4	4	4	4	4	4	4	4	4	4	4	4	4	4	4	4	4	4	4	4	4	5	5	4	4
4	4	4	1	2	2	4	4	4	4	4	4	4	4	4	4	4	3	2	3	4	4	4	4	4	4	4	4	5	5	4	4
4	4	2	1	2	2	4	4	4	4	4	4	4	4	4	4	4	3	3	2	4	4	4	4	4	4	4	4	5	5	4	4
4	4	2	1	2	2	4	4	4	4	4	4	4	4	4	4	4	4	3	2	2	4	4	4	4	4	4	4	4	5	5	4
4	4	3	1	2	4	4	4	4	4	4	4	4	4	4	4	4	3	3	2	1	4	4	4	4	4	4	4	4	5	5	4
4	4	2	1	2	4	4	4	4	4	4	4	4	4	4	4	3	3	2	2	1	2	4	4	4	4	4	4	4	5	5	4
4	4	2	1	2	4	4	4	4	4	4	4	4	4	4	4	4	4	3	2	2	4	4	4	4	4	4	4	4	5	5	4
4	4	1	1	2	4	4	4	4	4	4	4	4	4	4	4	4	3	2	2	1	1	4	4	4	4	4	4	4	5	5	4
2	4	1	1	2	4	4	4	4	4	4	4	4	4	4	5	4	4	4	4	2	1	4	4	4	4	4	4	4	5	5	5
1	4	1	1	3	4	4	4	4	4	4	4	4	4	4	4	4	4	4	4	1	1	4	4	4	4	4	4	4	4	5	5
1	1	1	1	3	4	3	4	4	3	4	3	4	4	5	4	4	4	3	3	2	1	4	4	4	4	4	4	4	4	5	5
1	1	1	1	3	3	3	4	3	3	3	3	3	3	4	4	4	4	3	3	2	2	4	3	4	3	3	4	3	4	5	5
1	1	1	1	3	1	2	2	3	3	3	3	3	4	5	5	5	4	4	4	2	2	3	3	2	2	2	3	3	4	5	5
1	1	1	1	4	4	4	4	4	4	4	4	4	3	5	4	4	4	4	4	2	2	1	4	4	4	4	4	4	4	4	4
1	1	1	4	3	3	4	3	4	2	4	4	4	4	3	3	4	4	4	4	3	4	2	4	[illegible]	4	4	4	3	4	4	4
1	1	1	1	4	4	4	4	4	2	3	3	4	4	3	4	4	4	4	4	3	4	1	2	4	4	4	4	4	4	4	4
1	1	1	1	1	4	4	2	4	1	2	3	4	4	2	2	2	1	4	1	2	3	1	1	2	1	2	4	3	3	4	2
1	1	1	2	1	4	4	2	4	1	1	2	3	4	4	2	2	1	4	1	3	3	1	1	1	1	1	3	4	3	4	4

FIGURE 13: CLUSTER STRUCTURE OF GRAYNESS CLASS NO. 5

The 1,024 points in the picture matrix were separated into the five performance classes. The table below shows the number of points per class, and the percentage of the total number of points in each class.

Class Number	Number of Points	Percentage of Total Points
1	74	7.23
2	82	8.01
3	77	7.52
4	744	72.66
5	47	4.59
	1,024	100.

By far the greatest number of points is in Class 4, which is the gray level that includes all of the sky (see Figure 7).

Initially, the matrix information was input to the cluster analysis row-by-row, from top left to bottom right. However, for subsequent clustering analyses, the points within each of the five classes were randomly presented. This enabled the clustering algorithm to exploit its ability to locate regions of interest. Additionally, avoiding a row-by-row analysis emphasized the contrast between encoding by clustering and encoding by Fourier transforms. The reconstructed picture for the cluster analysis is shown in Figure 14.

5.3 Fourier Transform Results

For the Fourier analyses, the picture was transformed and encoded row-by-row, resulting in 32 sets of coefficients, each set containing 32 coefficients. The picture was reconstructed in five ways, each using the following number of coefficients:

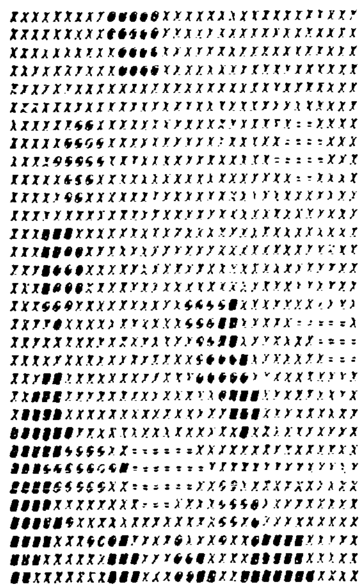

FIGURE 14: RECONSTRUCTION OF PICTURE FROM CLUSTER STRUCTURE

Reconstruction Number	Number of Coefficients (out of 32 max.)
1	31
2	29
3	23
4	15
5	7

In all cases, the highest frequency coefficients were eliminated; this means that the data were low-pass (spatial) filtered. Since the first two reconstructions are very similar to the original transform both in number of coefficients and in reconstruction accuracy, only the last three were considered extensively. Their reconstructions are shown in Figures 15 through 17.

5.4 Comparison of Results

The subjective accuracy of the cluster reconstructed pictures is less than that of any of the Fourier reconstructions. However, this is probably attributable to the coarseness of the digitization and the resulting large size of the clusters -- particularly those in Class 4 (as shown in Figure 12).

Various objective measures of accuracy enable more quantitative comparisons to be made. To begin with, it is important to consider the reduction in transmitted information achieved by each of the algorithms. The amount of data initially available is 1,024 "performance values" (i.e., gray levels).

The amount of information transmitted after clustering is equal to two scalars for each one-point cell (location coordinates) and four scalars for each larger cell (two location coordinates and two size factors). The amount of information transmitted by the Fourier transform method is the product of the number of rows and the number of coefficients retained per row. Table 12 lists the reduction in information volume for the cluster analysis and the last three Fourier analyses. There are two ways of describing the

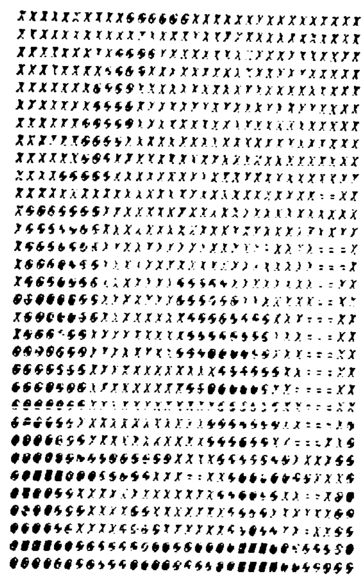

FIGURE 15: RECONSTRUCTION OF PICTURE FROM FOURIER TRANSFORM (7 LOW FREQUENCY COEFFICIENTS RETAINED)

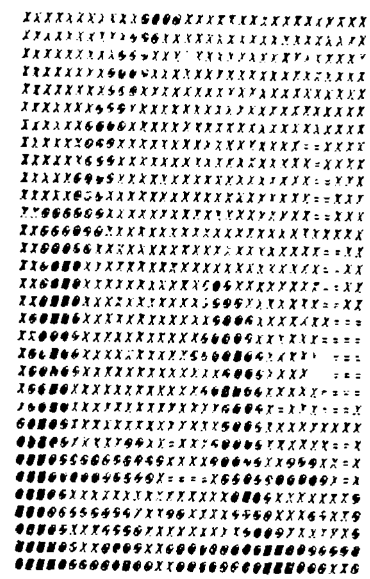

FIGURE 16: RECONSTRUCTION OF PICTURE FROM FOURIER TRANSFORM (15 LOW FREQUENCY COEFFICIENTS RETAINED)

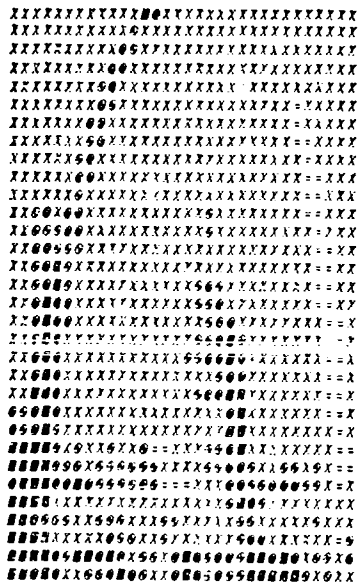

FIGURE 17: RECONSTRUCTION OF PICTURE FROM FOURIER TRANSFORM (23 LOW FREQUENCY COEFFICIENTS RETAINED)

TABLE 12

REDUCTION AND COMPRESSION OF INFORMATION
BY VARIOUS ENCODING METHODS

Method of Encoding Information	Number of Data Cells (N)	Reduction Factor (1-N/1024)	Compression Factor (1024/N)
Original Picture	1,024	0.00	1.00
Cluster	604	0.41	1.70
Fourier 3	736	0.28	1.39
Fourier 4	480	0.53	2.13
Fourier 5	224	0.78	4.57

reduction of information: one is the reduction factor, the fraction of original information that has been eliminated

$$R = 1 - \frac{N}{1024}$$

where N is the number of scalars transmitted for a given reconstruction; the second is the compression factor, the ratio of original information to transmitted information

$$C = \frac{1024}{N} .$$

The cluster analysis compares favorably to the Fourier analyses; its reduction in information falls between the third and fourth Fourier transforms.

Another way of assessing reconstructions is by comparing their relative accuracies point-by-point for the 1,024 points. Table 13 shows "confusion matrices" and resultant percentage accuracy for each of the four reconstructions. Again, the cluster reconstruction compares favorably; its accuracy is only slightly less than that of the fourth Fourier transform.

Figures 18 and 19 summarize the results of the two tables. The accuracy of the cluster results falls about 7 percent below that which would be expected from a (hypothetical) Fourier encoding with the same reduction and compression factors.

These results are very encouraging, particularly in view of two considerations: First, the limited range of the performance classes is more favorable to the Fourier method than to clustering. The clustering algorithm can readily deal with almost any number of gray levels; but given a wide range of values to model, the smoothing effect of a truncated Fourier transform would tend to eliminate the extreme values, which might be the most informative.

TABLE 13

CONFUSION MATRICES OF VARIOUS IMAGE RECONSTRUCTIONS

(a) FFT, 7 Coefficients Retained

True Class Value	Computed Class Value 1	2	3	4	5
1	11	45	18	0	0
2	0	25	53	4	0
3	3	6	53	15	0
4	0	11	133	574	26
5	0	0	5	26	16

66.3 Percent Accuracy

(b) FFT, 15 Coefficients Retained

True Class Value	Computed Class Value 1	2	3	4	5
1	33	39	2	0	0
2	8	51	21	2	0
3	0	8	59	10	0
4	0	4	71	656	13
5	0	0	0	11	36

81.5 Percent Accuracy

(c) FFT, 23 Coefficients Retained

True Class Value	Computed Class Value 1	2	3	4	5
1	54	20	0	0	0
2	8	62	12	0	0
3	0	2	69	6	0
4	0	0	24		3
5	0	0	0	4	43

92.3 Percent Accuracy

(d) Cluster of 1,024 Randomized Points

True Class Value	Computed Class Value 1	2	3	4	5
1	57	3	4	5	0
2	17	48	8	9	0
3	1	11	43	21	1
4	8	31	40	638	27
5	0	0	0	10	7

80.4 Percent Accuracy

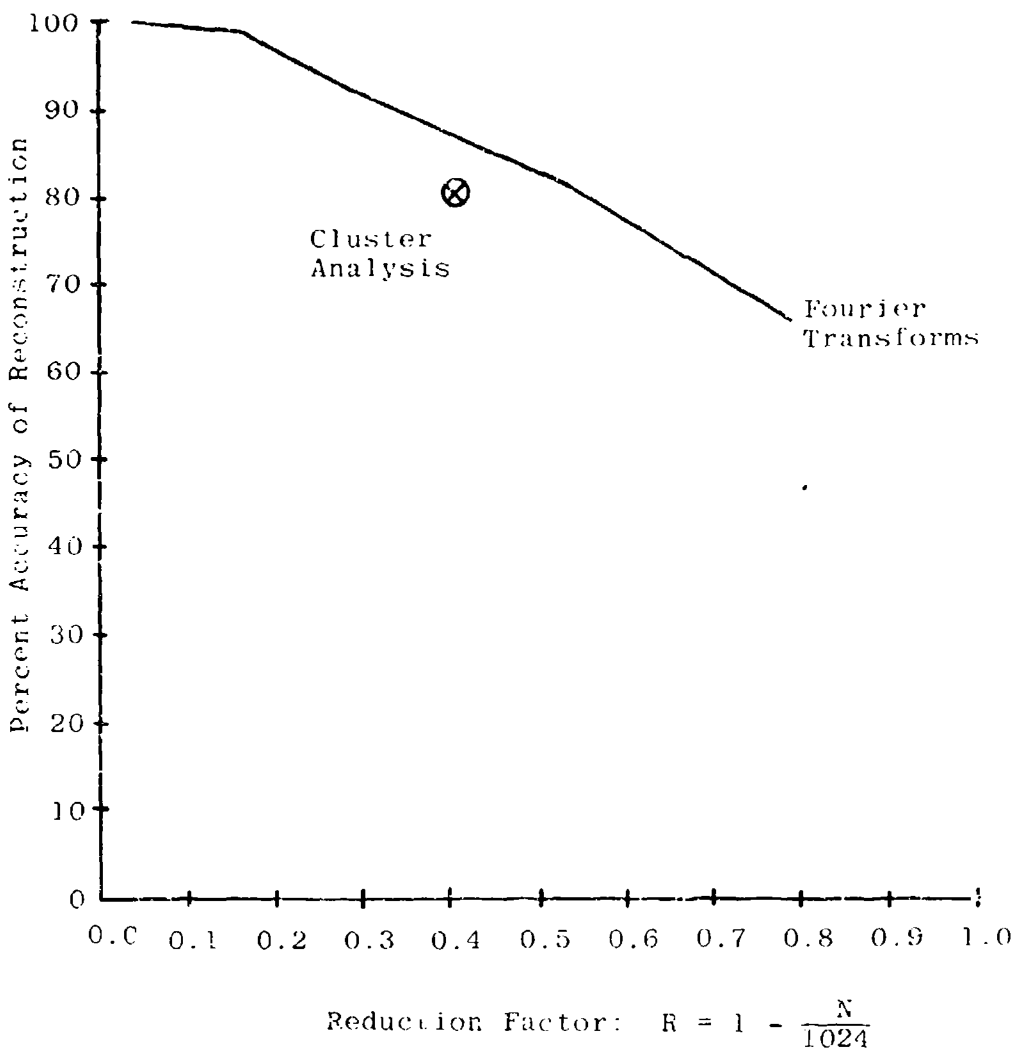

FIGURE 18: IMAGE RECONSTRUCTION ACCURACY AS A FUNCTION OF INFORMATION REDUCTION FOR TWO RECONSTRUCTION PROCEDURES

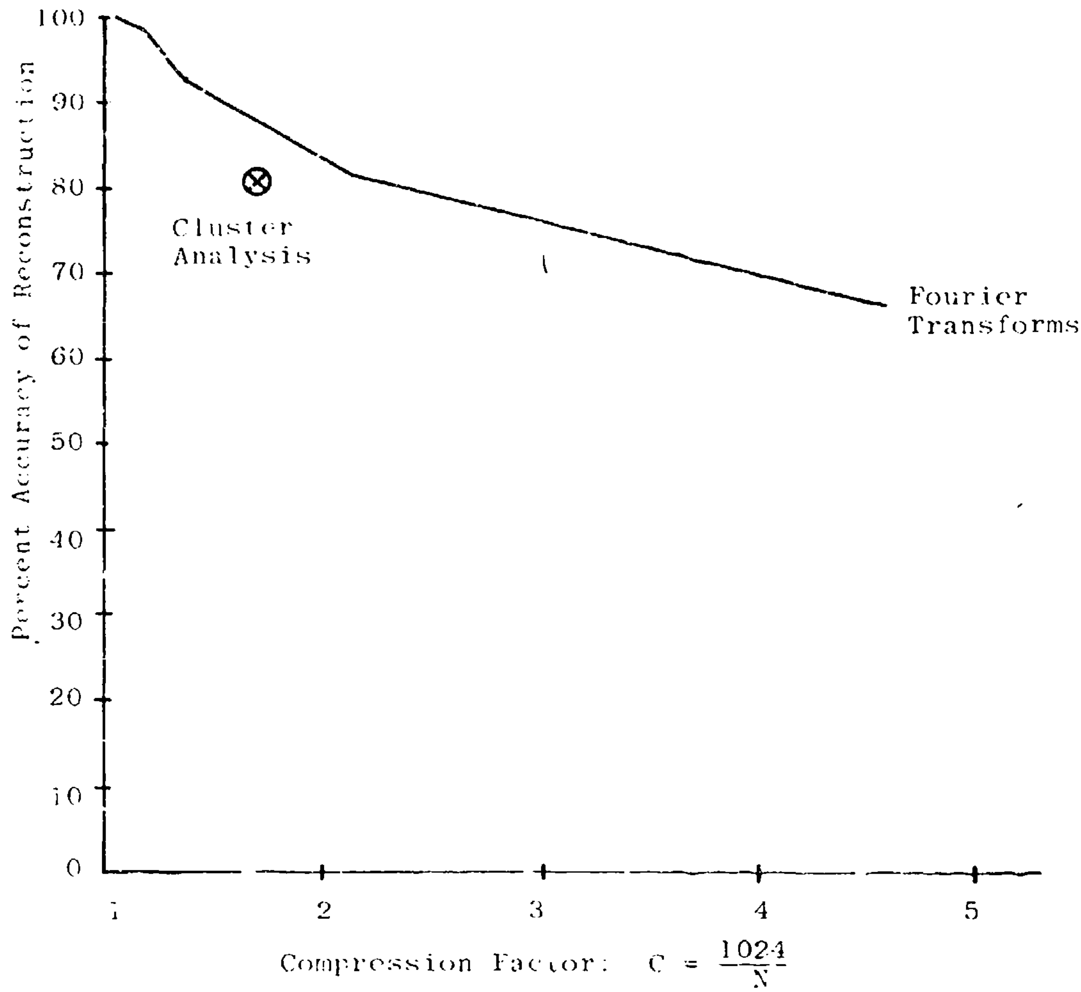

FIGURE 19: IMAGE RECONSTRUCTION ACCURACY AS A FUNCTION OF INFORMATION COMPRESSION FOR TWO RECONSTRUCTION PROCEDURES

Second, the reconstruction from clusters used here was an arbitrary and very simple method. There are several other methods to choose from; for example, computing the performance of each point as a weighted sum of the values of the nearest clusters or even of all the clusters. A more sophisticated reconstruction procedure could increase the accuracy of reconstruction from clusters well above that from a Fourier transform with the same volume of information.

5.5 Conclusions

Clustering analysis is certainly worth consideration as a method of image encoding and reconstruction. On a problem involving a very coarse sample size (32x32), reconstruction from clusters using a simple technique was only slightly less accurate than reconstruction via a Fourier transform with roughly the same reduction of information volume. In addition to providing a good reconstruction, clustering analysis can find regions of possible interest within the image because of its ability to consider the image as a whole rather than row-by-row. This characteristic considerably enhances its value as a tool in image pattern recognition and classification.

SECTION VI
CONCLUSIONS AND RECOMMENDATIONS

The work effort in this study has been devoted to extension and further development of search algorithms of utility for self-organizing control systems relevant to Air Force needs. Applications of these algorithms have demonstrated their capabilities for use in optimization of the parameters of human factors models that describe characteristics of man-machine interface problems.

The results of this study can be summarized as follows

- Search methods developed in the previous study have been extended to higher-dimensional, multimodal problems and have been shown to be very effective.
- A composite search algorithm incorporating both the pdf-guided search and the guided accelerated random search has been simulated and found to be more effective than either search algorithm alone.
- Clustering analysis for assessing the complexity of a search surface has shown to be of value.
- A new method for image encoding has been formulated that appears to be potentially superior to methods currently in use.

Further work should be initiated to seek ways of making current techniques more powerful, and to broaden their areas of application. We recommend that the following areas be investigated:

- Extensive effort should be devoted to developing an algorithm that combines the best features of PDF and GARS. The substitution of PDF for the first portion of GARS has been demonstrated to be an effective strategy. The next step should be to combine them into a single algorithm and to insert PDF into the statistically biased search phases of GARS so that its multimodal pdf model, which extends throughout the performance space, can be used to guide GARS in the choice of trial points, rather than the present unimodal pdf model. Additionally, provision should be made to explore local maxima as well as the global maximum, should this be desirable.

- The use of clustering analysis to measure the complexity of a search (optimization) problem should be examined more closely. A technique is needed that will make the cluster results more readily understood as a measure of complexity. This is especially important in problems of high dimensionality, where interpretation of clustering results can be difficult.

- The use of clustering analyses to encode and reconstruct images should be developed using pictures with finer divisions. A reconstruction function should be formulated that will take more advantage of the benefits to be gained from clustering -- in particular its sensitivity to regions of interest in the picture. The latter ability will directly couple this new encoding technique to pattern recognition/classification interests.

SECTION VII
REFERENCES

1. Andrews, H. C., A. G. Tescher and R. P. Kruger, "Image Processing by Digital Computer," IEEE Spectrum, July 1972, pp. 20-32.

2. Barron, R. L., "Parameter Space Search Techniques for Learning Automata," Proc. 1966 Bionics Symposium, Dayton, Ohio, May 1966.

3. Barron, R. L., "Inference of Vehicle and Atmosphere Parameters from Free-Flight Motions," J. Spacecrafts and Rockets, 6, June 1969, pp. 641-648.

4. Haralick, R. M., "Glossary and Index to Remotely Sensed Image Pattern Recognition Concepts," Pattern Recognition, 5, 1973, pp. 391-403.

5. Haralick, R. M., K. Shanmugam and I. Dinstein, "Textural Features for Image Classification," IEEE Trans. Systems, Man and Cybernetics, Vol. SMC-3, No. 6, November 1973, pp. 610-621.

6. Harmon, L. D. and B. Julesz, "Masking in Visual Recognition: Effects of Two-Dimensional Filtered Noise," Science, Vol. 180, June 15, 1973, pp. 1194-1196.

7. Idelsohn, J. M., "A Learning System for Terrain Recognition," Bendix Technical Journal, Spring 1972, pp. 33-38.

8. MacLeod, I. D. G., "Pictorial Output With A Line Printer," IEEE Trans. Computers, Vol. C-19, No. 2, February 1970, pp. 160-162.

9. Mucciardi, A. N., "Neuromime Nets as the Basis for the Predictive Component of Robot Brains," in Cybernetics, Artificial Intelligence, and Ecology, Robinson and Knight (eds.), Washington: Spartan Books, 1972, pp. 159-193.

10. Mucciardi, A. N. and E. E. Gose, "An Automatic Clustering Algorithm and Its Properties in High-Dimensional Spaces," IEEE Trans. Systems, Man and Cybernetics, Vol. SMC-2, April 1972, pp. 247-254.

11. Mucciardi, A. N., E. C. Orr, E. R. Johnson, and R. L. Barron, Investigation of the Theoretical Foundations of Self-Organizing and Learning Systems, Adaptronics, Inc., McLean, Va., AMRL-TR-73-76, Aerospace Medical Research Laboratory, W-PAFB, Ohio, December, 1973.

12. Mucciardi, A. N., "A New Class of Search Algorithms for Adaptive Computation," Proc. 12th IEEE Conf. on Decision and Control, San Diego, CA, December 1973, pp. 94-100.

13. Mucciardi, A. N. "Self-Organizing Probability State Variable Parameter Search Algorithms for Systems That Must Avoid High-Penalty Operating Regions," IEEE Trans. Systems, Man and Cybernetics, Vol. SMC-4, No. 4, July 1974, pp. 350-362.

APPENDIX A

SUMMARY OF RUNS 1 - 42 OF SECTION 3.5

TABLE A-1

RUN #	1	2	3	4
# OF DIMENSIONS	2	2	2	2
INITIAL RESOURCES	400.	400.	400.	400.
RESOURCE PER DIMENSION	200.	200.	200.	200.
PDF1				
# OF TRIALS	50	50	100	100
TRIALS PER DIMENSION	25	25	50	50
RESOURCE CONSUMED	52.60	52.60	103.87	103.87
% OF RESOURCE CONSUMED	13.15	13.15	25.97	25.97
BEST VALUE ACHIEVED	0.9897	0.9897	0.9897	0.9897
% OF MAXIMUM VALUE	97.4	97.4	97.4	97.4
ND†	0.02	0.02	0.02	0.02
PDF2				
# OF CLUSTERS	12	12	23	23
PDF3				
# OF TRIALS	500	500	440	440
TRIALS PER DIMENSION	250	250	220	220
RESOURCE CONSUMED	347.40	347.40	296.13	296.13
% OF RESOURCE CONSUMED	86.85	86.85	74.03	74.03
BEST VALUE ACHIEVED	1.0155	1.0155	1.0162	1.0162
% OF MAXIMUM VALUE	99.9	99.9	100.0	100.0
ND	0.00	0.00	0.00	0.00
IMPROVEMENT OVER PDF1#	0.0258	0.0258	0.0265	0.0265

GARS

	Run 1 ITER*	SUC.	BEST	%MAX	ND	Run 2 ITER	SUC.	BEST	%MAX	ND	Run 3 ITER	SUC.	BEST	%MAX	ND	Run 4 ITER	SUC.	BEST	%MAX	ND
PART 1	—	—	—	—	—	—	—	—	—	—	—	—	—	—	—	—	—	—	—	—
2	50	0	NI	NI	NI	50	1	1.001	99.4	0.01	50	0	NI	NI	NI	50	3	0.9952	97.9	0.02
3	50	0	NI	NI	NI	50	0	NI	NI	NI	50	0	NI	NI	NI	50	2	1.0012	98.5	0.02
4	50	1	1.0158	99.9	0.03	50	1	1.0156	99.9	0.00	50	1	1.0162	100.0	0.00	50	4	1.0155	99.9	0.00
5	20	1	1.0161	100	0.00	20	1	1.0163	100	0.00	20	0	NI	NI	NI	20	3	1.0164	100.0	0.00
OVERALL	170	2	..	..	..	170	3	..	..	..	170	1	1.0162	100.0	0.00	170	12	..	..	..
IMPROVEMENT OVER PDF	0.0009					0.0009					0.0000					0.0002				

† ND = NORMALIZED DISTANCE FROM BEST POINT TO GLOBAL MAXIMUM. NORMALIZED BY MAXIMUM DIAMETER OF SPACE, i.e., $(\text{NUMBER OF DIMENSIONS})^{\frac{1}{2}} \cdot 2$

* ITER = # OF ITERATIONS ALLOWED
SUC = # OF SUCCESSFUL TRIALS
BEST = BEST VALUE ACHIEVED
% MAX = % OF MAXIMUM VALUE

IMPROVEMENT = DIFFERENCE IN FUNCTION VALUES OF BEST POINTS, i.e., $\text{BEST}_{PDF3} - \text{BEST}_{PDF1}$

TABLE A-2

RUN #	5	6	7	8
# OF DIMENSIONS	2	2	2	2
INITIAL RESOURCES	400.	400.	400.	400.
RESOURCE PER DIMENSION	200.	200.	200.	200.
PDF1				
# OF TRIALS	200	200	200	200
TRIALS PER DIMENSION	100	100	100	100
RESOURCE CONSUMED	210.32	210.32	210.32	210.32
% OF RESOURCE CONSUMED	52.58	52.58	52.58	52.58
BEST VALUE ACHIEVED	0.9897	0.9897	0.9897	0.9897
% OF MAXIMUM VALUE	97.4	97.4	97.4	97.4
ND[†]	0.02	0.02	0.02	0.02
PDF2				
# OF CLUSTERS	48	48	48	48
PDF3				
# OF TRIALS	300	300	300	300
TRIALS PER DIMENSION	150	150	150	150
RESOURCE CONSUMED	189.68	189.68	189.68	189.68
% OF RESOURCE CONSUMED	47.12	47.12	47.42	47.42
BEST VALUE ACHIEVED	1.0141	1.0141	1.0141	1.0141
% OF MAXIMUM VALUE	99.8	99.8	99.8	99.8
ND	0.01	0.01	0.01	0.01
IMPROVEMENT OVER PDF1	0.0244	0.0244	0.0244	0.0244

GARS

RUN #	5					6					7					8				
	ITER*	SUC.	BEST	%MAX	ND	ITER.	SUC.	BEST	%MAX	ND	ITER.	SUC.	BEST	%MAX	ND	ITER.	SUC.	BEST	%MAX	ND
PART 1	—	—	—	—	—	—	—	—	—	—	—	—	—	—	—	—	—	—	—	—
2	50	0	NI	NI	NI	50	4	0.9906	97.5	0.02	50	1	0.9600	99.4	0.02	50	7	0.9811	96.5	0.03
3	50	0	NI	NI	NI.	50	2	0.9967	98.1	0.02	50	2	1.0050	98.9	0.01	50	1	0.9858	97.0	0.03
4	50	6	1.0152	99.9	0.00	50	4	1.0158	99.9	0.00	50	3	1.0154	99.9	0.00	50	7	1.0157	99.9	0.00
5	20	2	1.0164	100.0	0.00	20	1	1.0164	100.0	0.00	20	1	1.0165	100.0	0.00	20	1	1.0164	100.0	0.00
OVERALL	170	8	"	"	"	170	11	"	"	"	170	7	"	"	"	170	16	"	"	"
IMPROVEMENT OVER PDF	0.0023					0.0023					0.0022					0.0023				

[†] ND = NORMALIZED DISTANCE FROM BEST POINT TO GLOBAL MAXIMUM. NORMALIZED BY MAXIMUM DIAMETER OF SPACE, i.e., $(\text{NUMBER OF DIMENSIONS})^{\frac{1}{2}} \cdot 2$

3-8

* ITER = # OF ITERATIONS ALLOWED
SUC = # OF SUCCESSFUL TRIALS
BEST = BEST VALUE ACHIEVED
% MAX = % OF MAXIMUM VALUE

IMPROVEMENT = DIFFERENCE IN FUNCTION VALUES OF BEST POINTS, i.e., $BEST_{PDF3} - BEST_{PDF1}$

TABLE A-3

RUN #	9	10	11	12
# OF DIMENSIONS	2	2	2	2
INITIAL RESOURCES	400.			
RESOURCE PER DIMENSION	200.			
PDF1				
# OF TRIALS	200			
TRIALS PER DIMENSION	100			
RESOURCE CONSUMED	210.32			
% OF RESOURCE CONSUMED	52.58			
BEST VALUE ACHIEVED	0.9897			
% OF MAXIMUM VALUE	97.4			
ND+	0.02			
PDF2				
# OF CLUSTERS	48			
PDF3				
# OF TRIALS	300			
TRIALS PER DIMENSION	150			
RESOURCE CONSUMED	169.68			
% OF RESOURCE CONSUMED	47.42			
BEST VALUE ACHIEVED	1.0141			
% OF MAXIMUM VALUE	99.8			
ND	0.01			
IMPROVEMENT OVER PDF1#	0.0244			

GARS

	Run 9 ITER*	SUC.	BEST	% MAX	ND	Run 10 ITER.	SUC.	BEST	% MAX	ND	Run 11 ITER.	SUC.	BEST	% MAX	ND	Run 12 ITER.	SUC.	BEST	% MAX	ND
PART 1	—	—	—	—	—	20	4	0.5328	57.3	0.16	20	4	0.5828	57.3		20	5	0.5828	57.3	
2	50	3	1.0112	99.5	0.01	50	5	0.9640	94.8	0.02	20	3	0.9171	90.2		20	3	0.9171	90.2	
3	50	0	NI	NI	NI	50	1	0.9995	98.3	0.02	20	2	0.9847	96.9		20	2	0.9849	96.9	
4	50	2	1.0157	99.9	0.01	50	4	1.0157	99.9	0.00	20	4	1.0162	100.0		20	4	1.0159	99.9	
5	20	1	1.0164	100.0	0.00	20	1	1.0162	100.0	0.00	20	2	1.0164	100.0	0.00	20	2	1.0164	100.0	0.00
OVERALL	170	6	"	"	"	190	15	"	"	"	100	15	"	"	"	100	16	"	"	0.00
IMPROVEMENT OVER PDF	0.0023																			

+ ND = NORMALIZED DISTANCE FROM BEST POINT TO GLOBAL MAXIMUM. NORMALIZED BY MAXIMUM DIAMETER OF SPACE, i.e., $(\text{NUMBER OF DIMENSIONS})^{\frac{1}{2}} \cdot 2$

* ITER = # OF ITERATIONS ALLOWED
SUC. = # OF SUCCESSFUL TRIALS
BEST = BEST VALUE ACHIEVED
% MAX. = % OF MAXIMUM VALUE

IMPROVEMENT = DIFFERENCE IN FUNCTION VALUES OF BEST POINTS, i.e., $BEST_{PDF3} - BEST_{PDF1}$

3-9

TABLE A-4

RUN #	13	14	15	16
# OF DIMENSIONS	5	5	5	5
INITIAL RESOURCES	400.	400.	400.	400.
RESOURCE PER DIMENSION	80.	30.	80.	80.
PDF1				
# OF TRIALS	100	100	100	200
TRIALS PER DIMENSION	20	20	20	40
RESOURCE CONSUMED	100.36	100.36	100.36	194.10
% OF RESOURCE CONSUMED	25.09	25.09	25.09	48.52
BEST VALUE ACHIEVED	0.6365	0.6365	0.6365	0.6365
% OF MAXIMUM VALUE	65.65	65.65	65.65	65.65
ND†	0.16	0.16	0.16	0.16
PDF2				
# OF CLUSTERS	23	23	23	49
PDF3				
# OF TRIALS	367	367	367	259
TRIALS PER DIMENSION	73.4	73.4	73.4	51.8
RESOURCE CONSUMED	299.64	299.64	299.64	205.90
% OF RESOURCE CONSUMED	74.91	74.91	74.91	51.48
BEST VALUE ACHIEVED	0.7987	0.7987	0.7987	0.7654
% OF MAXIMUM VALUE	82.37	82.37	82.32	78.94
ND	0.10	0.10	0.10	0.12
IMPROVEMENT OVER PDF1	0.1622	0.1622	0.1622	0.1289

GARS

RUN #	13					14					15					16				
	ITER*	SUC.	BEST	%MAX	ND	ITER	SUC.	BEST	%MAX	ND	ITER	SUC.	BEST	%MAX	ND	ITER	SUC.	BEST	%MAX	ND
PART 1	—	—	—	—	—	—	—	—	—	—	—	—	—	—	—	—	—	—	—	—
2	50	2	0.8395	85.6		125	5	0.7555	77.9		50	4	0.8105	83.6		50	0	NI	NI	NI
3	50	5	0.9127	99.1		125	12	0.9662	99.6		50	10	0.9403	97.0		50	2	0.9142	94.3	
4	50	9	0.9691	99.9		125	3	.9692			50	9	0.9693	99.9		50	12	0.9691	99.9	
5	50	6	0.9696	100.0	0.00	50	5	0.9696	100.0	0.00	50	5	0.9696	100.0	0.00	50	3	0.9685	100.0	0.00
OVERALL	200	22	"	"	0.00	425	25	"	"	"	200	28	"	"	0.00	200	17	"	"	"
IMPROVEMENT OVER PDF	0.1709					0.1709					0.1709					0.2041				

† ND = NORMALIZED DISTANCE FROM BEST POINT TO GLOBAL MAXIMUM. NORMALIZED BY MAXIMUM DIAMETER OF SPACE, i.e., $(\text{NUMBER OF DIMENSIONS})^{\frac{1}{2}} \cdot 2$

* ITER. = # OF ITERATIONS ALLOWED
SUC. = # OF SUCCESSFUL TRIALS
BEST = BEST VALUE ACHIEVED
% MAX. = % OF MAXIMUM VALUE

‡ IMPROVEMENT = DIFFERENCE IN FUNCTION VALUES OF BEST POINTS, i.e., $BEST_{PDF3} - BEST_{PDF1}$

3-10

TABLE A-5

RUN #	17	18	19	20
# OF DIMENSIONS	5	5	5	5
INITIAL RESOURCES	400.	400.	400.	400.
RESOURCE PER DIMENSION	80.	80.	80.	80.
PDF1				
# OF TRIALS	200	200	200	200
TRIALS PER DIMENSION	40	40	40	40
RESOURCE CONSUMED	194.10	194.10	194.10	194.10
% OF RESOURCE CONSUMED	48.52	48.52	48.52	48.52
BEST VALUE ACHIEVED	0.6365	0.6365	0.6365	0.6365
% OF MAXIMUM VALUE	65.65	65.65	65.65	65.65
ND†	0.16	0.16	0.16	0.16
PDF2				
# OF CLUSTERS	49	49	49	49
PDF3				
# OF TRIALS	259	259	259	259
TRIALS PER DIMENSION	51.8	51.8	51.8	51.8
RESOURCE CONSUMED	205.90	205.90	205.90	205.90
% OF RESOURCE CONSUMED	51.48	51.48	51.48	51.48
BEST VALUE ACHIEVED	0.7654	0.7654	0.7659	0.7654
% OF MAXIMUM VALUE	78.94	78.94	78.94	78.94
ND	0.12	0.12	0.12	0.12
IMPROVEMENT OVER PDF1	^ 1289	0.1289	0.1289	0.1289

GARS

Run 17:

	ITER*	SUC.	BEST	%MAX	ND
PART 1	—	—	—	—	—
2	50	7	0.6377	65.8	
3	50	11	0.9568	98.7	
4	50	3	0.9695	100.0	
5	50	5	0.9696	"	0.00
OVERALL	200	26	"	"	"
IMPROVEMENT OVER PDF	0.2042				

Run 18:

	ITER	SUC.	BEST	%MAX	ND
PART 1	—	—	—	—	—
2	50	2	0.5463	56.3	
3	50	11	0.9271	95.6	
4	50	12	0.9693	100.0	
5	50	2	0.9696	"	0.00
OVERALL	200	27	"	"	0.00
IMPROVEMENT OVER PDF	0.2042				

Run 19:

	ITER	SUC.	BEST	%MAX	ND
PART 1	—	—	—	—	—
2	50	2	0.7848	80.9	
3	50	7	0.9621	99.2	
4	50	3	0.9694	100.0	
5	50	5	0.9696	"	0.00
OVERALL	200	22	"	"	0.00
IMPROVEMENT OVER PDF	0.2012				

Run 20:

	ITER	SUC.	BEST	%MAX	ND
PART 1	—	—	—	—	—
2	50	8	0.7254	74.8	
3	50	5	0.9424	97.2	
4	50	8	0.9692	100.0	
5	50	4	0.9696	"	0.00
OVERALL	200	25	"	"	"
IMPROVEMENT OVER PDF	0.2042				

† ND = NORMALIZED DISTANCE FROM BEST POINT TO GLOBAL MAXIMUM. NORMALIZED BY MAXIMUM DIAMETER OF SPACE, i.e., $(\text{NUMBER OF DIMENSIONS})^{\frac{1}{2}} \cdot 2$

* ITER = # OF ITERATIONS ALLOWED
SUC. = # OF SUCCESSFUL TRIALS
BEST = BEST VALUE ACHIEVED
% MAX. = % OF MAXIMUM VALUE

†† IMPROVEMENT = DIFFERENCE IN FUNCTION VALUES OF BEST POINTS, i.e., $BEST_{PDF3} - BEST_{PDF1}$

3-11

TABLE A-6

RUN #	21	22	23	24
# OF DIMENSIONS	5	5	5	5
INITIAL RESOURCES	400.	400.	400.	400.
RESOURCE PER DIMENSION	80.	80.	80.	80.
PDF1				
# OF TRIALS	200	200	200	200
TRIALS PER DIMENSION	40	40	40	40
RESOURCE CONSUMED	194.10	194.10	194.10	194.10
% OF RESOURCE CONSUMED	48.52	48.52	48.52	48.52
BEST VALUE ACHIEVED	0.6365	0.6365	0.6365	0.6365
% OF MAXIMUM VALUE	65.65	65.65	65.65	65.65
ND†	0.16	0.16	0.16	0.16
PDF2				
# OF CLUSTERS	49	49	49	49
PDF3				
# OF TRIALS	259	259	259	259
TRIALS PER DIMENSION	51.8	51.8	51.8	51.8
RESOURCE CONSUMED	205.90	205.90	205.90	205.90
% OF RESOURCE CONSUMED	51.48	51.48	51.48	51.48
BEST VALUE ACHIEVED	0.7654	0.7654	0.7654	0.7654
% OF MAXIMUM VALUE	78.99	78.99	78.99	78.99
ND	0.12	0.12	0.12	0.12
IMPROVEMENT OVER PDF1	0.1289	0.1289	0.1289	0.1289

GARS

	21 ITER*	SUC.	BEST	%MAX	ND	22 ITER	SUC.	BEST	%MAX	ND	23 ITER	SUC.	BEST	%MAX	ND	24 ITER	SUC.	BEST	%MAX	ND
PART 1	—	—	—	—	—	—	—	—	—	—	—	—	—	—	—	—	—	—	—	—
2	50	5	0.9471	97.7		50	2	0.8306	85.7		50	6	0.4965	51.2		50	8	0.5099	52.6	
3	50	1	0.9561	98.6		50	8	0.9275	95.9		50	13	0.9595	99.0		50	2	0.5477	56.5	
4	50	5	0.9662	100.0		50	5	0.9691	99.9		50	4	0.9662	100.0		50	11	0.5496	56.7	
5	50	2	0.9696	"	0.00	50	5	0.96[illegible]	100.0	0.00	50	5	0.9696	"	0.00	50	5	0.5499	"	0.37
OVERALL	200	13	"	"	0.00	200	20	"	"	0.00	200	28	"	"	0.00	200	26	"	"	"
IMPROVEMENT OVER PDF	0.2042					0.2042					0.2042					-0.2155				

† ND = NORMALIZED DISTANCE FROM BEST POINT TO GLOBAL MAXIMUM. NORMALIZED BY MAXIMUM DIAMETER OF SPACE, i.e., $(\text{NUMBER OF DIMENSIONS})^{\frac{1}{2}} \cdot 2$

* ITER = # OF ITERATIONS ALLOWED
SUC. = # OF SUCCESSFUL TRIALS
BEST = BEST VALUE ACHIEVED
% MAX. = % OF MAXIMUM VALUE

\# IMPROVEMENT = DIFFERENCE IN FUNCTION VALUES OF BEST POINTS, i.e., $BEST_{PDF3} - BEST_{PDF1}$

3-12

TABLE A-7

RUN #	25	26	27	28
# OF DIMENSIONS	5	10	10	10
INITIAL RESOURCES		400	400	400
RESOURCE PER DIMENSION		40	40	40
PDF1				
# OF TRIALS		100	100	200
TRIALS PER DIMENSION		10	10	20
RESOURCE CONSUMED		98.54	98.54	193.52
% OF RESOURCE CONSUMED		24.64	24.64	48.38
BEST VALUE ACHIEVED		0.6526	0.6526	0.6526
% OF MAXIMUM VALUE		68.99	68.90	68.99
ND+		0.13	0.13	0.13
PDF2				
# OF CLUSTERS		14	14	23
PDF3				
# OF TRIALS		351	351	250
TRIALS PER DIMENSION		35.1	35.1	25.0
RESOURCE CONSUMED		301.46	301.46	206.48
% OF RESOURCE CONSUMED		75.34	75.34	51.62
BEST VALUE ACHIEVED		0.6526	0.6526	0.6526
% OF MAXIMUM VALUE		68.99	68.99	68.99
ND		0.13	0.13	0.13
IMPROVEMENT OVER PDF1		0.00	0.00	0.00

GARS

	25 ITER*	SUC.	BEST	%MAX	ND	26 ITER.	SUC.	BEST	%MAX	ND	27 ITER.	SUC.	BEST	%MAX	ND	28 ITER.	SUC.	BEST	%MAX	ND
PART 1	50	6	0.4191	43.2		—	—	—	—	—	—	—	—	—	—	—	—	—	—	—
2	50	6	0.7130	73.5		100	5	0.7867	82.5		250	12	0.7347	77.7	0.11	100	5	0.7807	82.5	
3	50	7	0.9477	97.7		100	13	0.9318	98.5		250	17	0.9441	99.8	0.01	100	13	0.9318	98.5	
4	50	9	0.9692	100.0		100	4	0.9455	100.0		250	9	0.9454	99.9	0.01	100	4	0.9455	100.0	
5	50	3	0.9690	"	0.00	100	10	0.9459	"	0.00	100	10	0.9159	100.0	0.00	100	10	0.9459	"	0.00
OVERALL	250	31	"	"	"	400	32	"	"	0.00	850	48	"	"	0.00	400	32	"	"	0.00
IMPROVEMENT OVER PDF#						0.2933					0.2933					0.2933				

+ ND = NORMALIZED DISTANCE FROM BEST POINT TO GLOBAL MAXIMUM. NORMALIZED BY MAXIMUM DIAMETER OF SPACE, i.e., $(\text{NUMBER OF DIMENSIONS})^{\frac{1}{2}} \cdot 2$

* ITER. = # OF ITERATIONS ALLOWED
SUC. = # OF SUCCESSFUL TRIALS
BEST = BEST VALUE ACHIEVED
% MAX. = % OF MAXIMUM VALUE

\# IMPROVEMENT = DIFFERENCE IN FUNCTION VALUES OF BEST POINTS, i.e., $BEST_{PDF3} - BEST_{PDF1}$

TABLE A-8

RUN #	29	30	31	32
# OF DIMENSIONS	10	10	10	15
INITIAL RESOURCES	400.	400.		600.
RESOURCE PER DIMENSION	40.	40.		40.
PDF1				
# OF TRIALS	200	200		200
TRIALS PER DIMENSION	20	20		13.3
RESOURCE CONSUMED	193.52	193.52		213.18
% OF RESOURCE CONSUMED	48.38	98.38		35.53
BEST VALUE ACHIEVED	0.6526	0.6526		0.4017
% OF MAXIMUM VALUE	68.99	68.99		41.58
ND[+]	0.13	0.13		0.21
PDF2				
# OF CLUSTERS	23	23		31
PDF3				
# OF TRIALS	250	250		424
TRIALS PER DIMENSION	25.0	25.0		28.3
RESOURCE CONSUMED	206.48	206.48		386.82
% OF RESOURCE CONSUMED	51.62	51.62		64.47
BEST VALUE ACHIEVED	0.6526	0.6526		0.6850
% OF MAXIMUM VALUE	68.99	68.99		70.91
ND	0.13	0.13		0.14
IMPROVEMENT OVER PDF1	0.00	0.00		0.2833

GARS	29					30					31					32				
	ITER*	SUC.	BEST	%MAX	ND	ITER.	SUC.	BEST	%MAX	ND	ITER.	SUC.	BEST	%MAX	ND	ITER.	SUC.	BEST	%MAX	ND
PART 1	—	--	—	—	—	—	—	—	—	—	100	3	0.3042	32.1	—	—	--	—	—	—
2	100	5	0.5894	62.2		100	5	0.6014	63.6		100	10	0.7218	76.3		150	4	0.7210	74.6	
3	100	21	0.9135	96.6		100	14	0.7779	82.2		100	17	0.9240	97.7		150	31	0.9521	98.6	
4	100	3	0.9452	100.0		100	7	0.7928	83.8		100	6	0.9455	100.0		150	16	0.9654	99.9	
5	100	15	0.9459	"	0.00	100	11	0.7933	83.9	0.37	100	10	0.9459	"	0.00	150	19	0.9659	100.0	0.00
OVERALL	400	44	"	"	0.00	400	37	"	"	"	500	46	"	"	"	600	70	"	"	"
IMPROVEMENT OVER PDF	0.2933					0.1407										0.2809				

[+] ND = NORMALIZED DISTANCE FROM BEST POINT TO GLOBAL MAXIMUM. NORMALIZED BY MAXIMUM DIAMETER OF SPACE, i.e., $(\text{NUMBER OF DIMENSIONS})^{\frac{1}{2}} \cdot 2$

3.14

* ITER = # OF ITERATIONS ALLOWED
SUC = # OF SUCCESSFUL TRIALS
BEST = BEST VALUE ACHIEVED
% MAX = % OF MAXIMUM VALUE

[++] IMPROVEMENT = DIFFERENCE IN FUNCTION VALUES OF BEST POINTS, i.e., $BEST_{PDF3} - BEST_{PDF1}$

TABLE A-9

RUN #	33	34	35	36
# OF DIMENSIONS	15	15	15	15
INITIAL RESOURCES	600.	600	600.	
RESOURCE PER DIMENSION	40	40	40	
PDF1				
# OF TRIALS	200	200	200	
TRIALS PER DIMENSION	13.3	13.3	13.3	
RESOURCE CONSUMED	213.18	213.18	213.18	
% OF RESOURCE CONSUMED	35.53	35.53	35.53	
BEST VALUE ACHIEVED	0.4017	0.4017	0.4017	
% OF MAXIMUM VALUE	41.58	41.58	41.58	
ND*	0.21	0.21	0.21	
PDF2				
# OF CLUSTERS	31	31	31	
PDF3				
# OF TRIALS	424	424	424	
TRIALS PER DIMENSION	28.3	28.3	28.3	
RESOURCE CONSUMED	386.82	386.82	386.82	
% OF RESOURCE CONSUMED	64.47	64.47	64.47	
BEST VALUE ACHIEVED	0.6850	0.6850	0.6850	
% OF MAXIMUM VALUE	70.91	70.91	70.91	
ND	0.14	0.14	0.14	
IMPROVEMENT OVER PDF1	0.2833	0.2833	0.2833	

GARS

RUN 33	ITER#	SUC.	BEST	%MAX	ND
PART 1	—	—	—	—	—
2	150	[illegible]	0.6193	64.1	
3	150	29	0.9525	98.6	
4	150	11	0.9645	99.9	
5	150	23	0.9660	100.0	0.00
OVERALL	600	70	"	"	"
IMPROVEMENT OVER PDF	0.2810				

RUN 34	ITER.	SUC.	BEST	%MAX	ND
PART 1	—	—	—	—	—
2	150	11	0.6451	66.8	
3	150	41	0.9587	99.2	
4	150	17	0.9650	100.0	
5	150	16	0.9660	"	0.00
OVERALL	600	85	"	"	"
IMPROVEMENT OVER PDF	0.2810				

RUN 35	ITER.	SUC.	BEST	%MAX	ND
PART 1	—	—	—	—	—
2	150	6	0.5653	58.5	
3	150	41	0.9450	97.8	
4	150	16	0.9650	100.0	
5	150	17	0.9660	"	0.00
OVERALL	600	80	"	"	0.00
IMPROVEMENT OVER PDF	0.2810				

RUN 36	ITER.	SUC.	BEST	%MAX	ND
PART 1	150	6	0.5450	56.4	
2	150	12	0.8118	84.0	
3	150	25	0.9559	99.0	
4	150	8	0.9650	100.0	
5	150	17	0.9660	"	0.00
OVERALL	750	68	"	"	"
IMPROVEMENT OVER PDF					

* ND = NORMALIZED DISTANCE FROM BEST POINT TO GLOBAL MAXIMUM. NORMALIZED BY MAXIMUM DIAMETER OF SPACE, i.e. (NUMBER OF DIMENSIONS)$^{\frac{1}{2}}\cdot 2$

\# ITER = # OF ITERATIONS ALLOWED
SUC = # OF SUCCESSFUL TRIALS
BEST = BEST VALUE ACHIEVED
% MAX = % OF MAXIMUM VALUE

\+ IMPROVEMENT = DIFFERENCE IN FUNCTION VALUES OF BEST POINTS, i.e., $BEST_{PDF3} - BEST_{PDF1}$

3-15

RUN #	37	38	39	40
# OF DIMENSIONS	20	20	20	20
INITIAL RESOURCES	600	600	600	600
RESOURCES PER DIMENSION	30	30	30	30
PDF1				
# OF TRIALS	200	200	200	200
TRIALS PER DIMENSION	10	10	10	10
RESOURCE CONSUMED	234.74	234.74	234.74	234.74
% OF RESOURCE CONSUMED	39.12	39.12	39.12	39.12
BEST VALUE ACHIEVED	0.2873	0.2873	0.2873	0.2873
% OF MAXIMUM VALUE	28.00	28.00	28.00	28.00
ND†	0.38	0.38	0.38	0.38
PDF2				
# OF CLUSTERS	32	32	32	32
PDF3				
# OF TRIALS	324	324	324	324
TRIALS PER DIMENSION	16.2	16.2	16.2	16.2
RESOURCE CONSUMED	365.26	365.26	365.26	365.26
% OF RESOURCE CONSUMED	60.88	60.88	60.88	60.88
BEST VALUE ACHIEVED	0.5280	0.5280	0.5280	0.5280
% OF MAXIMUM VALUE	51.47	51.47	51.47	51.47
ND	0.31	0.31	0.31	0.31
IMPROVEMENT OVER PDF1	0.2407	0.2407	0.2407	0.2407

GABS

	ITER* (37)	SUC.	BEST	%MAX	ND	ITER. (38)	SUC.	BEST	%MAX	ND	ITER. (39)	SUC.	BEST	%MAX	ND	ITER. (40)	SUC.	BEST	%MAX	ND
PART 1	—	—	—	—	—	—	—	—	—	—	—	—	—	—	—	—	—	—	—	—
2	200	20	0.766	66.0		500	37	0.717	69.9		500	39	0.6323	61.6		200	25	0.6482	63.2	
3	200	36	1.0034	97.3		500	92	1.0209	99.5		500	104	1.0250	90.9		200	44	0.9875	96.3	
4	200	3	1.0040	97.9		500	0	NI	NI		500	0	NI	NI		200	3	0.9889	96.4	
5	200	103	1.0258	100.0	0.00	200	81	1.0258	100.0	0.00	500	36	1.0259	100.0	0.00	200	200	1.0255	100.0	0.00
OVERALL	800	162	"	"	-	1700	210	-	-	-	1700	179	"	-	-	800	269	-	"	"
IMPROVEMENT OVER PDF††	0.4979					0.4978					0.4979									

† ND = NORMALIZED DISTANCE FROM BEST POINT TO GLOBAL MAXIMUM NORMALIZED BY MAXIMUM DIAMETER OF SPACE, i.e., (NUMBER OF DIMENSIONS)$^{\frac{1}{2}}$ 2

3-16

* ITER = # OF ITERATIONS ALLOWED
SUC = # OF SUCCESSFUL TRIALS
BEST = BEST VALUE ACHIEVED
% MAX = % OF MAXIMUM VALUE

†† IMPROVEMENT = DIFFERENCE IN FUNCTION VALUES OF BEST POINTS, i.e., $BEST_{PDF3} - BEST_{PDF1}$

TABLE A-11

RUN #	41	42		
# OF DIMENSIONS	20	20		
INITIAL RESOURCES				
RESOURCE PER DIMENSION				
PDF1				
# OF TRIALS				
TRIALS PER DIMENSION				
RESOURCE CONSUMED				
% OF RESOURCE CONSUMED				
BEST VALUE ACHIEVED				
% OF MAXIMUM VALUE				
ND†				
PDF2				
# OF CLUSTERS				
PDF3				
# OF TRIALS				
TRIALS PER DIMENSION				
RESOURCE CONSUMED				
% OF RESOURCE CONSUMED				
BEST VALUE ACHIEVED				
% OF MAXIMUM VALUE				
ND				
IMPROVEMENT OVER PDF1				

GARS	ITER*	SUC.	BEST	% MAX	ND	ITER	SUC.	BEST	% MAX	ND	ITER	SUC.	BEST	% MAX	ND	ITER	SUC.	BEST	% MAX	ND
PART 1	200	4	[illegible]	32.1		200	4	0.3290	32.1											
2	200	[illegible]	[illegible]	62.2		200	65	0.6035	62.2											
3	200	[illegible]	[illegible]	97.6		200	61	1.0011	97.6											
4	200	[illegible]	1.0012	"		200	3	1.0012	"											
5	200	153	1.0259	100.0	0.00	200	153	1.0259	100.0	0.00										
OVERALL	1000	236	"	"	"	1000	236	"	"	"										
IMPROVEMENT OVER PDF																				

† ND: NORMALIZED DISTANCE FROM BEST POINT TO GLOBAL MAXIMUM. NORMALIZED BY MAXIMUM DIAMETER OF SPACE, i.e. (NUMBER OF DIMENSIONS)$^{\frac{1}{2}}\cdot 2$

* ITER = # OF ITERATIONS ALLOWED
SUC = # OF SUCCESSFUL TRIALS
BEST = BEST VALUE ACHIEVED
% MAX = % OF MAXIMUM VALUE

\# IMPROVEMENT = DIFFERENCE IN FUNCTION VALUES OF BEST POINTS, i.e., $BEST_{PDF3} - BEST_{PDF1}$

3-17